1970

Fracture surface energy determinations of high density polycrystalline ceramics

Gene Arthur Pahlmann

Department:

1. Ceramic materials
I. Title

FRACTURE SURFACE ENERGY DETERMINATIONS OF HIGH DENSITY POLYCRYSTALLINE CERAMICS

BY

GENE ARTHUR PAHLMANN 1946 -

A

THESIS

submitted to the faculty of

UNIVERSITY OF MISSOURI-ROLLA

in partial fulfillment of the requirements for the Degree of

MASTER OF SCIENCE IN CERAMIC ENGINEERING

Rolla, Missouri

1970

Approved by

Robert C. Moore (Advisor)

Vincent J. Weidlich

David A. Summers

ABSTRACT

Values of fracture surface energy were measured for steatite, zircon, mullite and four densities of alumina.

Rods of these high density materials were cut into thin rectangular specimens which were notched and broken in three-point loading. The resulting load necessary for fracture of the specimens was used to calculate the fracture surface energy of the materials.

The value for the steatite was around 20,000 ergs/cm^2. The values for the zircon and mullite were on the order of 13,000 ergs/cm^2, and the values for the aluminas ranged from 17,000 to 24,000 ergs/cm^2.

ACKNOWLEDGMENTS

The author wishes to thank the following people for their assistance with his research:

First of all his advisor, Dr. Robert E. Moore, whose encouragement played a great role in his research and the writing of his thesis.

The unending and untiring advice and assistance from Dr. David A. Summers was tremendously helpful. Not only did Dr. Summers help him by his previous knowledge of the subject of fracture surface energy and its measurement; but without the use of Dr. Summers' equipment, the entire project might have ended in disaster.

The help of Mr. Richard Turner for the ΔT determinations, and the help of Mr. Richard Moore with the sonic apparatus for the Young's modulus determination are also appreciated.

The financial assistance of the Refractories Institute is acknowledged and appreciated.

TABLE OF CONTENTS

LIST OF FIGURES

Figures Page

LIST OF TABLES

SYMBOLS USED THROUGHOUT THESIS

I. For Surface Energy Determination:

γ = Fracture surface energy (ergs/cm^2)

σ = Stress in specimen

L = Length between loading supports (inches)

d = Width of specimen (inches)

x = The ratio (L/d)

b = Thickness of specimen (inches)

M = Bending moment in the specimen

c = Initial notch depth (inches)

y = Distance from neutral axis

$\frac{c}{d}$ = Notch depth to width ratio

p = Load required for fracture of specimen (psi)

E = Young's modulus (lbs/in^2)

L* = Length of sample

II. For Young's Modulus Determination:

C' = Shape factor term (sec^2/in)

ℓ = Length of sample (inches)

d = Diameter of specimen

f = Resonant frequency of specimen (cps)

T_1 = Correction factor

w = Weight of specimen (lbs-or-grams/454)

III. Additional Symbols:

ΔT = The amount of cooling shock (C^{o}) necessary to create surface cracking of the material

ρ = Density of material

I. INTRODUCTION

A recent specialized study of thermal shock in high density alumina by Ainsworth[1] prompted this extended study of thermal shock in other high density ceramic materials. Ainsworth's work dealt with the possibility of being able to predict the extent of thermal shock damage (the depth of cracks produced) in rods of the material as a result of exposure to a cooling shock of ΔT. In order to be able to use Ainsworth's equations it is necessary to obtain a valid, reproducible value for the fracture surface energy of the materials under examination. The determination of these surface energy values will be the main content of this thesis.

Fracture surface energy is the work required per unit area to create new surface. The density of the materials, type of bonding between particles, particle size and other material properties are responsible for the magnitude of this value.

The method used to determine these surface energy values was one similar to that described by Davidge and Tappin[2] and identical with that used by Summers.[3]

Since ½" x 6" rods of the materials were to be used for the thermal shock study, it was felt that it would be

advantageous to use similar rods for the surface energy determinations. These rods were sliced with a diamond saw and specimens of approximately 3/8" x .045" x 2" were made. These specimens were then notched with wire or diamond saw with notches ranging from 0.01" to 0.03" in width. They were then broken in 3-point bending; the center load being applied directly over the inverted notch. The applied load necessary for the fracture of the specimen was measured by a quartz load cell that was located directly in line and above the knife edge. The surface energy was then calculated by an equation given by Srawley.[4] The method of evaluation chosen made use of Griffith's crack theory. The final choice of an equation to be used for calculation of the fracture surface energy value was the result of the extensive experimentation of Summers[3] and Chen.[5]

II. REVIEW OF LITERATURE

A. Surfaces in General:

Boundary areas between phases are sometimes referred to as surfaces and are often the location of abrupt changes in composition, e.g. liquid-vapor interface, etc. For this reason atoms on or near these surfaces are not usually in equilibrium, since they are often not totally in either phase. This frequency results in many distorted bonds which in turn cause an excess of energy due to atoms which do not have all their bonds in equilibrium positions. Since the atomic surface structure is the cause of this population of unsatisfied bonds, this excess energy is proportional to the surface area. For this reason a drop of liquid will tend to form a spherical shape whenever possible, to minimize its surface area. (Producers of lead shot take advantage of this phenomenon by dropping molten lead through cool air. By the time the lead lands, it has hardened and will be quite spherical.)

Fracture surface energy is the energy required to produce a new surface.[6] Surface energy and surface tension tend to decrease with increasing temperature. The decrease in surface energy is the driving force for grain growth and sintering.[7]

B. Bonding and Strengths of Materials:

Weiderhorn[8] speaks of "theoretical cohesive strength" which could be used almost synonymously with fracture surface energy, (in idealized circumstances). In his study of glass and sapphire, he found their theoretical strengths to vary up to 100X greater than actual or normal engineering strength. In glass the theoretical strengths may be so much as three orders of magnitude greater than design strengths.

The maximum cohesive strength can be spoken of in terms of the binding energy between the atoms or molecules making up the structure. At a given interatomic distance, r_o, the binding potential of the material is at a maximum. When this distance is increased (or decreased), the binding potential decreases exponentially.

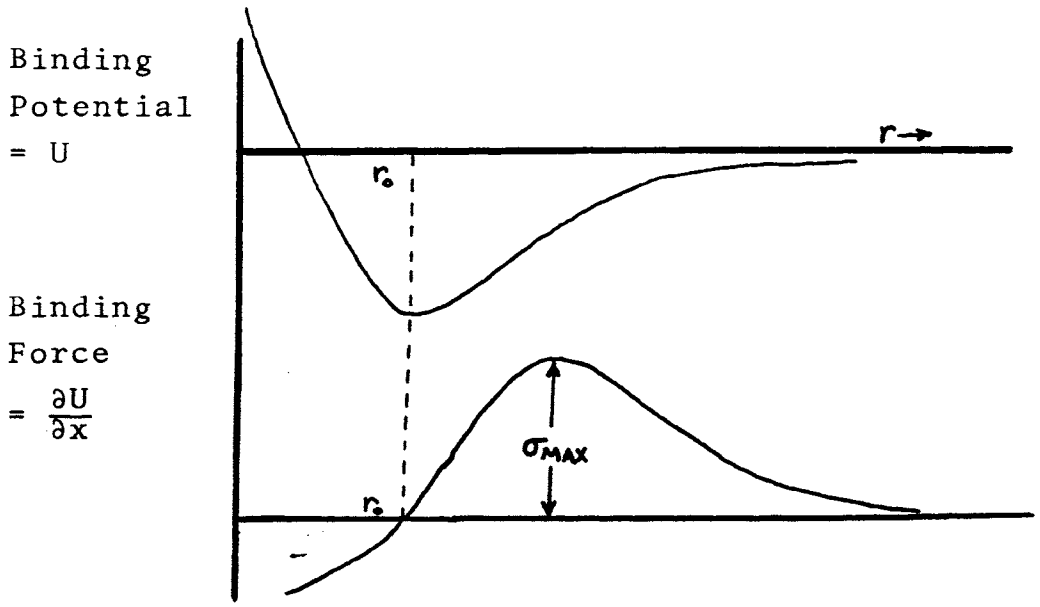

U equals the potential energy per unit area of fracture surface. Born's fraction describing U is:

$$U = \frac{-A}{x} + \frac{B}{x^n} \qquad (1)$$

The cohesive strength is calculated from the fact that $\frac{\partial^2 U}{\partial x^2} = 0$, when the stress is maximum. At equilibrium $x = x_o$ (i.e. r_o). By definition:

$$2\gamma = \int_{x_o}^{\infty} \sigma(x)dx = \int_{x_o}^{\infty} (\partial U/\partial x)dx = U]_{x_o}^{\infty} \qquad (2)$$

C. Flaw Theory of Fracture:

Since there is little or no mechanism in ceramic materials to allow plastic flow, the concentration of stresses at the tips of flaws cannot be relieved by plastic flow. For this reason the flaws act as stress concentrators, and, therefore, each flaw is a possible nucleation site for fracture. Most failure in ceramic materials is of a brittle nature and occurs with little or no warning.

In 1920 Griffith developed a theory that the main cause of fracture in brittle materials relates to a population of very small cracks (10-100 microns) within the body or on the surface especially, and these act as stress concentrators.

By using Ingles' analysis of stress, Griffith showed that the stress at the crack tip was:

$$\sigma = (2S\pi L/\rho)^{\frac{1}{2}} \tag{3}$$

Here L = ½ the length of the crack; ρ = the radius of curvature of the crack tip and S = the applied stress.

Griffith's famous equation for the stress (S) which is necessary for crack growth was that:

$$\text{S must equal or exceed: } (2E\gamma/L\pi)^{\frac{1}{2}} \tag{4}$$

By assuming a crack length in a material on the order of the interatomic spacing, one can calculate the rupture stress of Eq. (3) and obtain a magnitude compatible with that used for theoretical strength values. If the size of the flaw is on the order of 10-100 microns (Griffith type flaws), the strength values resulting are similar to those observed in actual applications. This would tend to strengthen Griffith's theory, if nothing else.

By examining the Griffith balance criteria ($\frac{-\partial U}{\partial A} = \gamma$) where U = the stored elastic energy and A = the fracture surface area, we see that when the requirements for this equation are fulfilled, crack growth is energetically possible. Once growth has begun, its behavior is dependent on how $\frac{-\partial U}{\partial A}$ changes with growth. A positive value for

$\frac{-\partial^2 U}{\partial A^2}$ will result in crack acceleration since the energy released is greater than that required for growth. If $\frac{-\partial^2 U}{\partial A^2}$ is negative, this may mean there will be a point during crack propagation at which $\frac{-\partial U}{\partial A} < \gamma$. If this occurs, crack growth will terminate and more work must be done to keep the crack moving.[9]

D. Methods of Surface Energy Measurement:

The most direct surface energy measurement is by determining the heat of solution or heat of reaction of very fine particles of known size. By dissolving or reacting this finely powdered material and measuring the change in temperature of the original bulk material, it is possible to make a direct calculation of the surface energy.[6]

Methods of crushing the sample and then measuring and/or calculating the resulting surface area have been studied by Kenny[11] and others. There is one very great difficulty that is always present in these crushing techniques viz., the powders must be strain free and free from surface contamination.[6] 'It is almost impossible to meet these two conditions simultaneously.'

E. Evaluation of Methods of Fracture Surface Energy Determination:

In Summers'[3] recent work, he compared and evaluated various methods for determination of fracture surface energy values. He explains that in a number of methods where the material is ground or crushed, many cracks may be formed within the resulting granules which are not readily visible or detectable. Since the number of these nondetected cracks will vary, crushing techniques will give not only high values of fracture surface energy but also inconsistent values. For his experimental material he chose plexiglas. Besides being quite homogeneous and readily available, it was a material that gave a smooth fracture plane that allowed accurate surface area measurements. Although the possibility of having some plastic behavior in this material is most apparent, the results should only deviate from a true fracture surface energy value by a constant term, so no real harm was done in using the plastic specimens to study "a brittle phenomenon." (His work was intended to evaluate methods rather than obtain standard values.)

Summers felt that using thin specimen sections and 3-point loading would help to reduce the level of stored

energy. His experiments were set up in four parts:

(1) The size of the specimens were varied but their dimensions were kept in constant proportion and sharpened notches were cut into the material to half the depth of the specimen.

(2) The specimens' dimensions were kept in constant proportion but three different notch shapes were used: (a) a vee notch, (b) a square ended notch, and (c) a round wire saw cut.

(3) The thickness and length being held constant, the crack to height ratio was varied at a constant total height.

(4) The crack to height ratio varied but the uncracked height remained constant.

The assumption upon which all work was based was that Griffith's theory of crack propagation holds true. For it to hold, Rose and English[5] have shown that for geometrically similar beams the relationship below must hold true:

$$\frac{p^2}{D^3} = (k) \cdot (\text{constant}) \qquad (5)$$

Here p = the applied load, D = a specimen dimension, and k has been related to the surface energy of the material. This implies that in order for fracture surface energy equation to be valid, the values calculated from it must

be constant over a wide range of sizes of materials tested and not for just one "special case."

By using the four sets of experimental variables already mentioned, Summers set out to examine the constancy of the values resulting from eight different fracture surface energy equations. Of the equations examined were those put forth by Liebowitz, Winne and Wundt, Paris and Sih, Buekner, Griffith, Davidge and Tappin, Srawley and Brown and Srawley.[3]

Three equations proved to be invalid when experimental changes in the initial crack length were made. Another gave way because its "qualifying assumptions" did not account for stored residual energy. Three others gave a wide range of values when the uncracked height was varied. This left only one of the original eight equations which gave quite constant values throughout the entire examination. This was the equation given by Srawley,[4] (which is discussed in detail in section five of this paper.)[5]

III. EXPERIMENTAL PROCEDURE

A. Materials Used:

The test specimens for this work were in the form of 6-inch rods, ½ inch in diameter. The materials examined were 99.5%, 96% and 94% dense alumina, steatite (ALSIMAG #460) and zircon (ALSIMAG #475) all donated by the American Lava Corporation; mullite (MV-30) donated by McDanel Refractories and 99% dense alumina (AD-99) which was purchased from Coors Porcelain. (A complete listing of addresses for materials and equipment used is included in the appendices.)

For the fracture surface energy specimens, the rods mentioned above were cut in half and then sliced into rectangular specimens of approximately 3/8" x .045" x 2" in dimensions. The specimens used in the ΔT determinations were round cylinders cut from the ½" rods and were slightly over an inch in length. For subsequent thermal shock studies, rods of 3 or 6 inch lengths will be used.

B. Procedure for Testing Specimens:

The rectangular specimens were placed in the loading jig (Fig. 1), and the knife edge of the jig was carefully lowered until it was centered above the inverted crack and

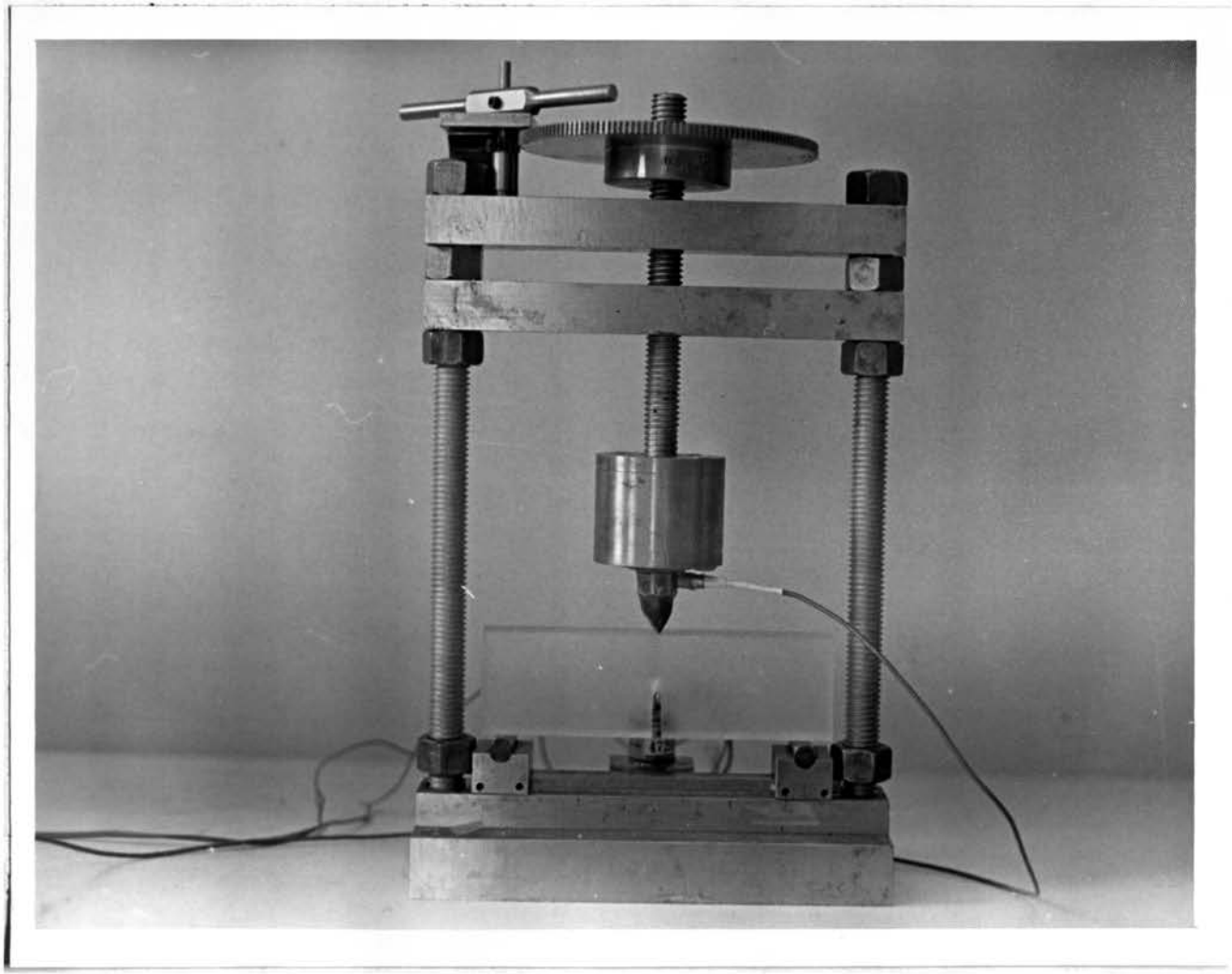

Figure 1: THE LOADING JIG

just barely in contact with the specimen. By observing the movement of the recorder, it was possible to determine when the knife edge no longer exerted pressure on the specimen.

The load was applied slowly and at a constant rate by use of the gears atop the loading jig. A double set of bearings allowed the shaft to rotate and descend while the knife edge remained stationary. When fracture occurred, in most cases, the specimens remained in one piece thus giving the assurance that very little of the input energy was elastic. Failure was considered to be of a completely brittle nature.

The recording of the load was accomplished by positioning a quartz load cell between the knife edge and the descending shaft. This load cell's range extended from 0.01 to 5,000 pounds of applied pressure. The output from this calibrated load cell was run through a charge amplifier which produced a signal that activated the recorder (one volt output per pound of applied pressure.)

The load taken from the recorder was used as the 'p' value in the following equation:

$$\gamma = \frac{9\pi p^2 L^2 c}{8Eb^2 d^4}\left[A_o + A_1\left(\frac{c}{d}\right) + A_2\left(\frac{c}{d}\right)^2 + A_3\left(\frac{c}{d}\right)^3 + A_4\left(\frac{c}{d}\right)^4\right]^2$$

$A_o = 1.9 + .0075x$, $A_1 = -3.39 + .08x$, $A_2 = 15.4 - .2175x$, $A_3 = -26.24 + .2815x$, $A_4 = 26.38 - .145x$

(Equation by Srawley[4]) (6)

C. Measurements and Calculations:

The values of: L, c, d and b were measured with a dial type micrometer. All the 'c' values were measured under a 16 power microscope. The accuracy of the micrometer was to the nearest thousandth of an inch.

The values for Young's modulus were measured by using the sonic techniques described by Pickett,[12] using the formula: $E = c'wf^2$, for calculations.

For an explanation of the terms used in this paper, one may refer to the listing at the beginning of the paper and also to the diagram on the following page.

The deflection of some of the specimens was measured using the LVDT attachment (Fig. 3). For most of the thin specimens, their deflection before fracture was only about 0.002 to 0.004" and this small flexure was felt to be so close to the limits of accuracy of the device that the values were not recorded.

After all the specimens were broken, the values were read off the chart paper under a magnifying lens to help insure that the readings would be accurate and consistent. The full scale readings on the recorder paper for all but a few very thick specimens were set from 5 to 20 pounds.

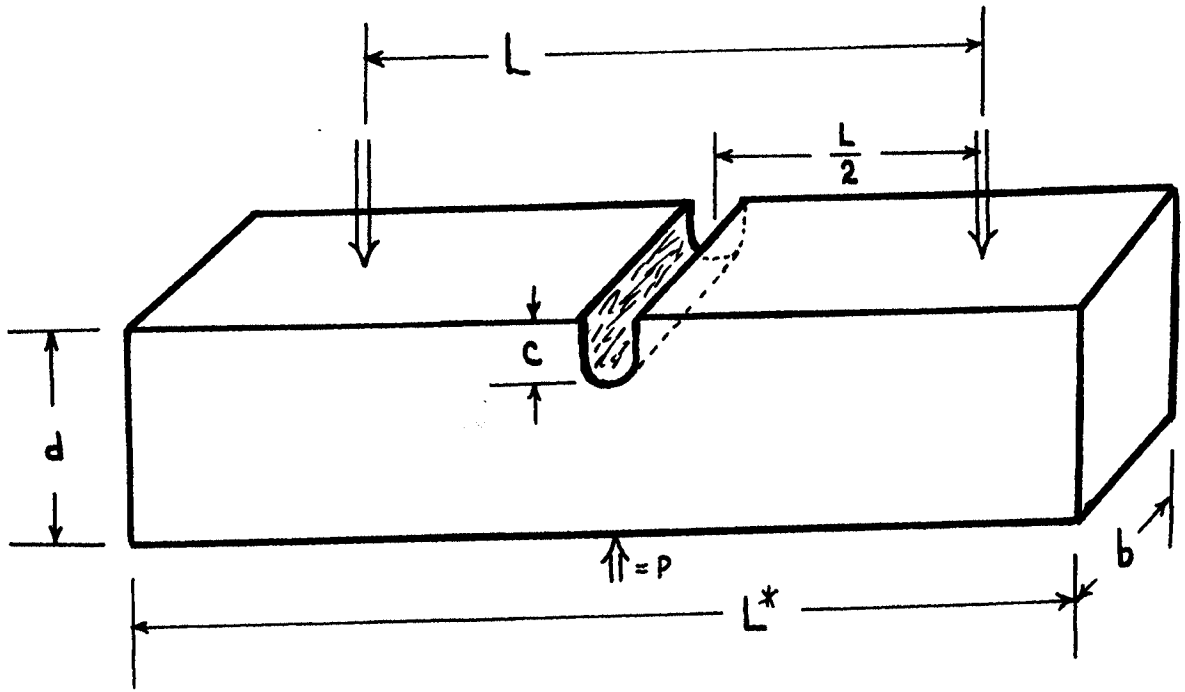

⇓ = load supports and applied load (p)

Figure 2: SPECIMEN DIMENSIONS

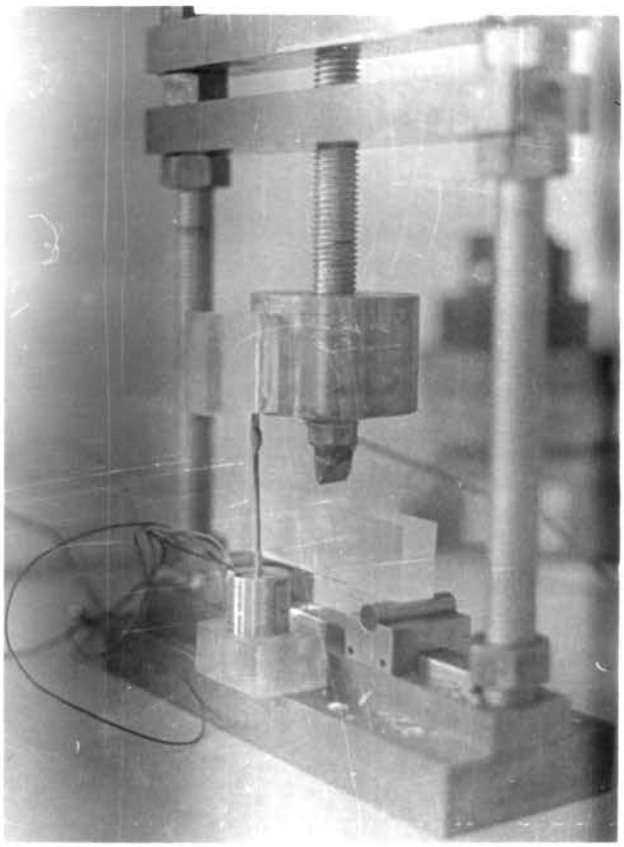

Figure 3: THE LVDT ATTACHMENT

These settings allowed a minimum accuracy in reading of ±0.01 pounds.

IV. RESULTS

Table I on the following page summarizes the data taken in this work. Appendix 'C' contains all the data taken on the seven different materials.

It was found that the three different densities of alumina from American Lava (94, 96 and 99.5% dense) gave fracture surface energy values which decreased with increasing density. Those average values were 24,269, 20,125 and 17,526 ergs/cm^2, respectively. The value obtained from the 99% dense alumina from Coors Porcelain gave us an average value of 24,184 ergs/cm^2. The steatite* gave an average value of 20,401 while the values for mullite** and zircon* were almost identical: 13,348 and 13,748 ergs/cm^2, respectively.

Figures 3 and 4 show the distinction between the cut and fractured surfaces of the aluminas. Figures 6 through 12 show photomicrographs of the fractured surfaces of all the materials studied. (Photos were taken with the scanning electron microscope.)

---

* From AMERICAN LAVA

** From MC DANEL REFRACTORIES

TABLE I

AVERAGE VALUES FROM EXPERIMENTAL FINDINGS

Material	Fracture Surface Energy	ΔT	Young's Modulus
99.5% Al_2O_3	17,526 ergs/cm^2	175C°	55 x 10^6psi*
99% Al_2O_3	24,184	215°	58.8 x 10^6
96% Al_2O_3	20,125	215°	51.8 x 10^6
94% Al_2O_3	24,269	215°	45.6 x 10^6**
Steatite	20,401	125°	16.1 x 10^6
Mullite	13,748	275°	23.6 x 10^6
Zircon	13,348	225°	26.5 x 10^6

* Value from American Lava Corporation

** (B-5), E = 53.4 x 10^6

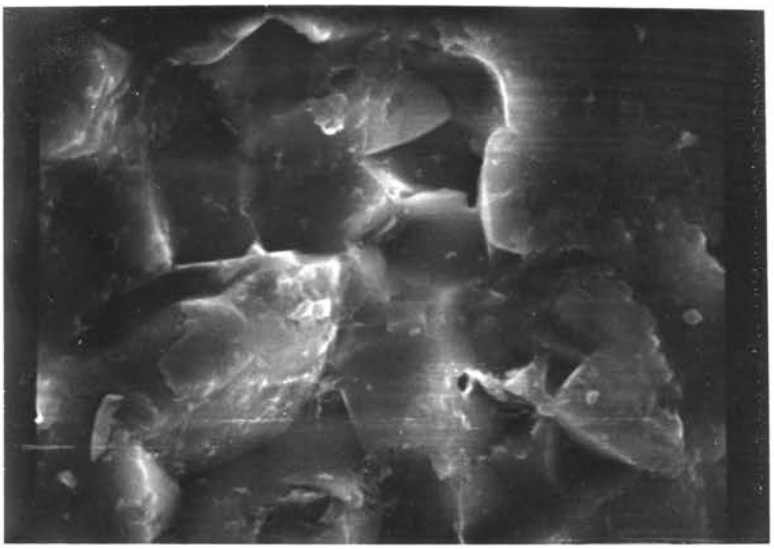

a) CUT SURFACE - 3000X

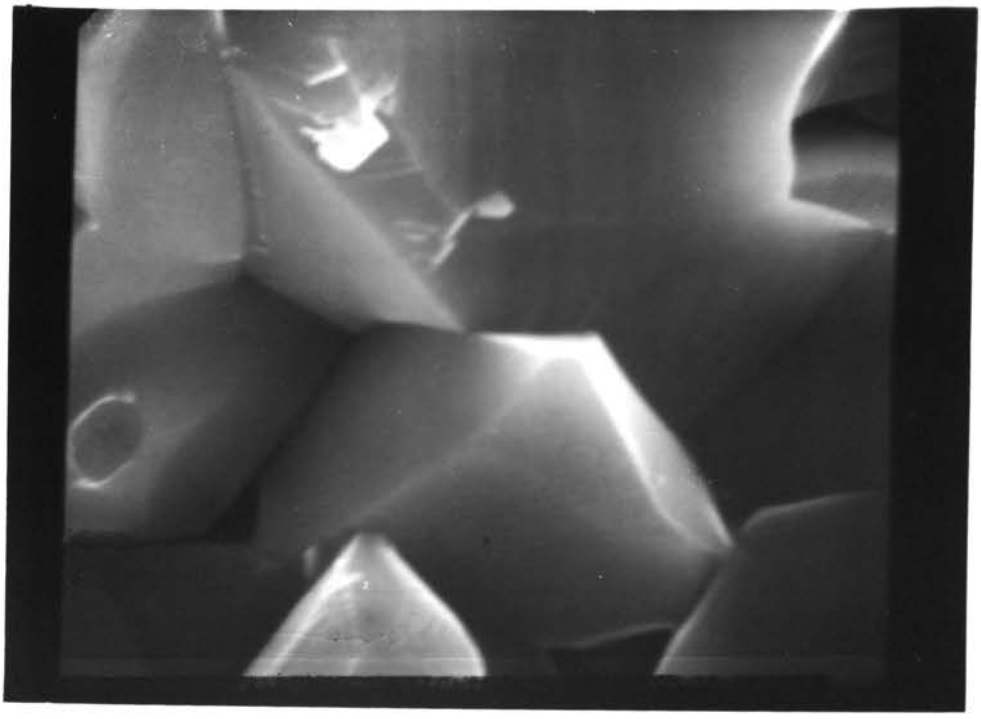

b) FRACTURED SURFACE - 5000X

Figure 4: ALUMINA (99% dense)

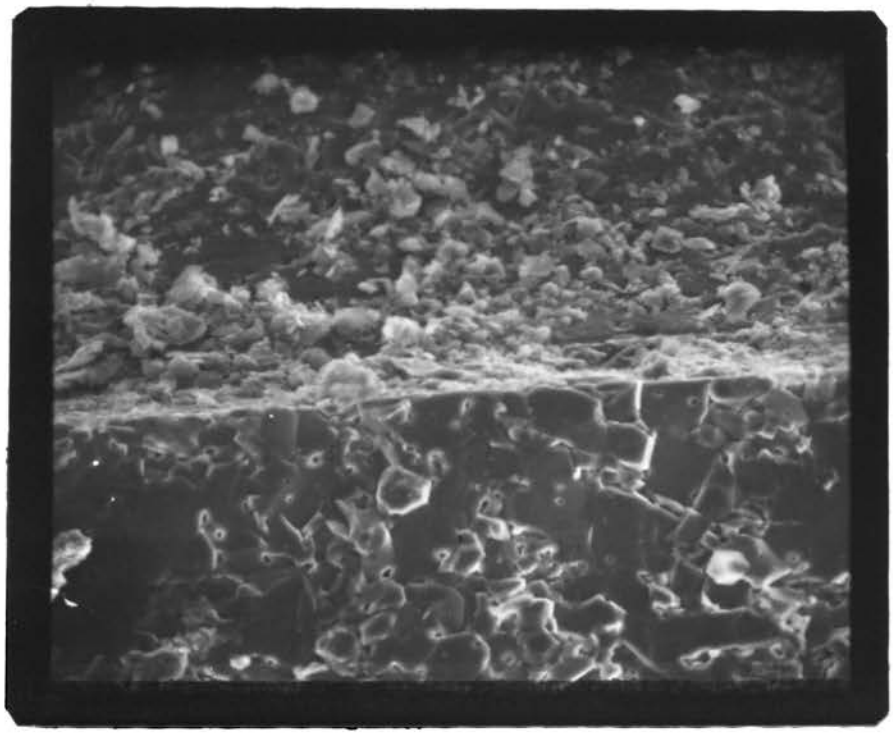

Figure 5: NOTCH-FRACTURE INTERFACE
(300X, 99.5% Alumina)
(Top half = cut portion)

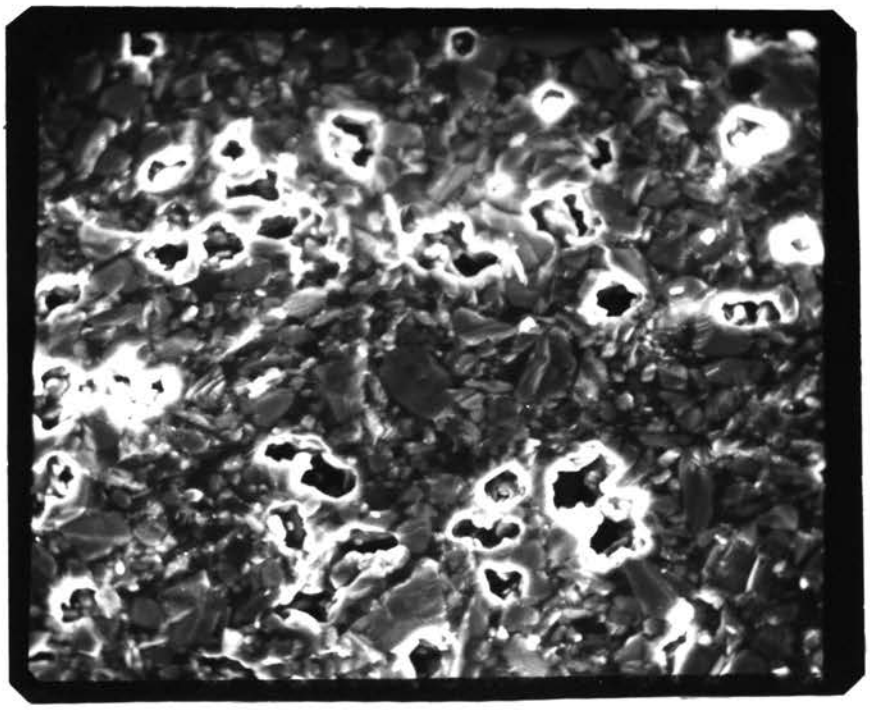

a) 500X

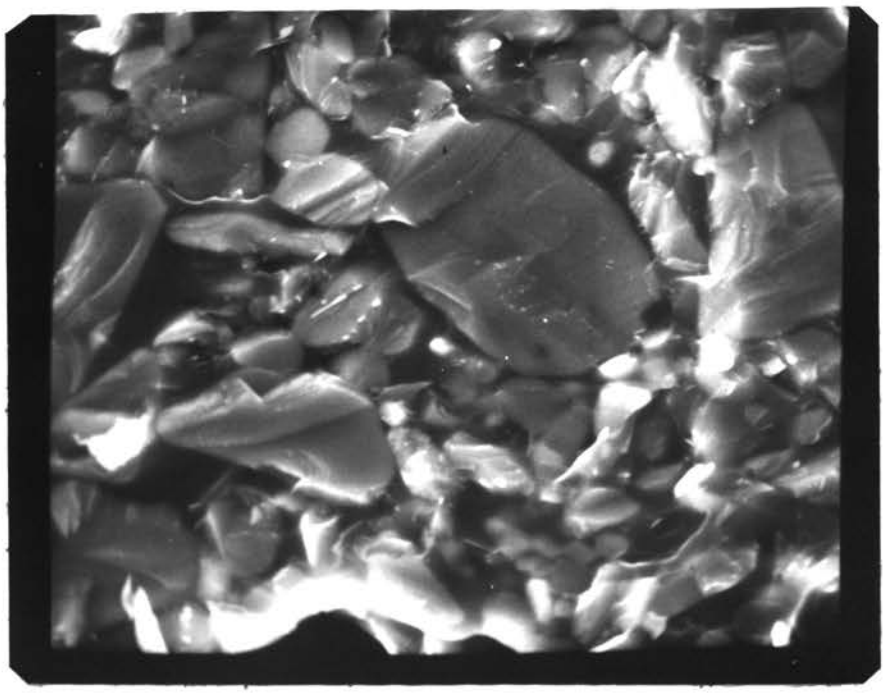

b) 1400X

Figure 6: ZIRCON FRACTURE SURFACE

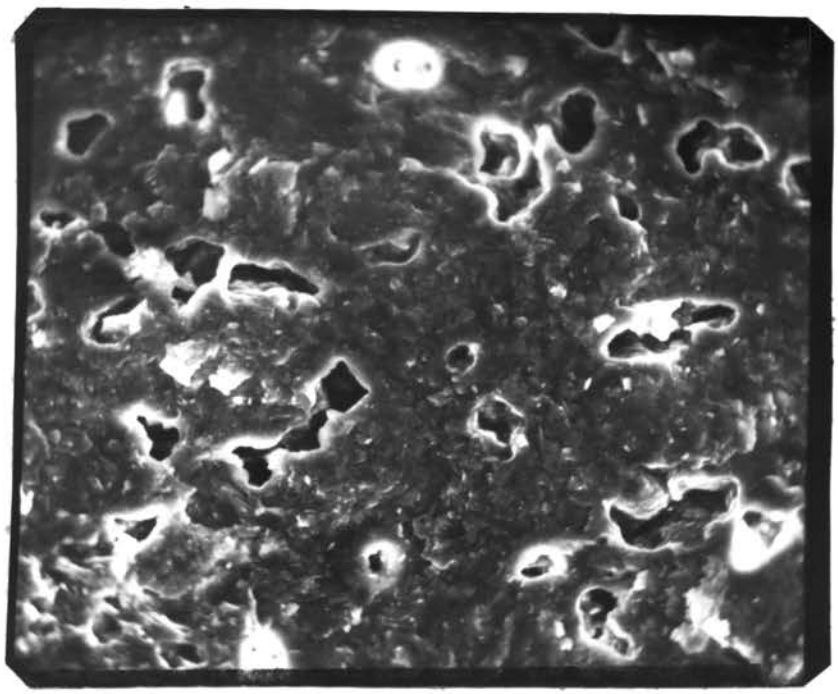

a) 500X

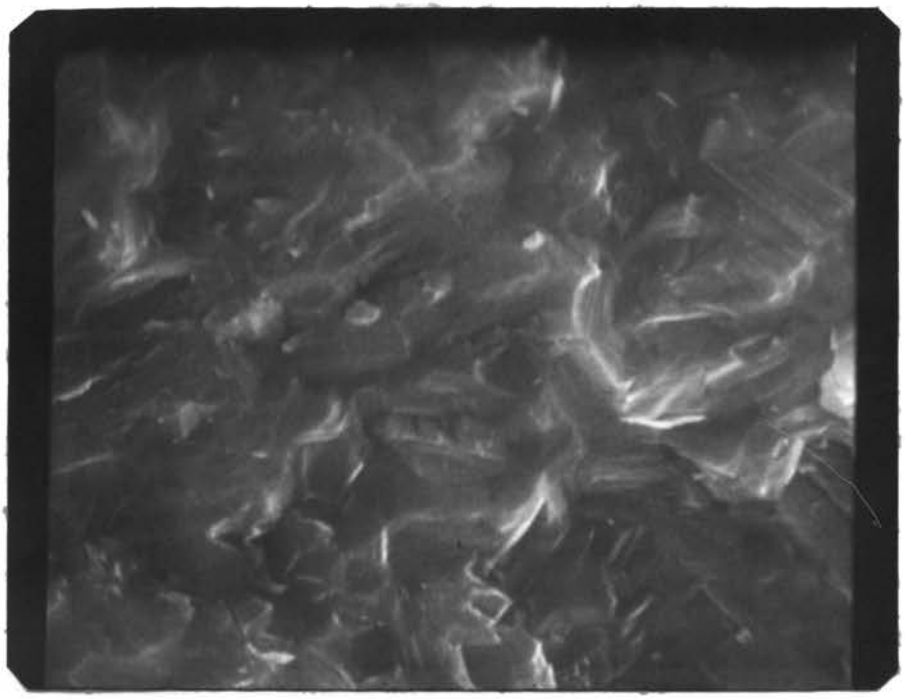

b) 5000X

Figure 7: STEATITE FRACTURE SURFACE

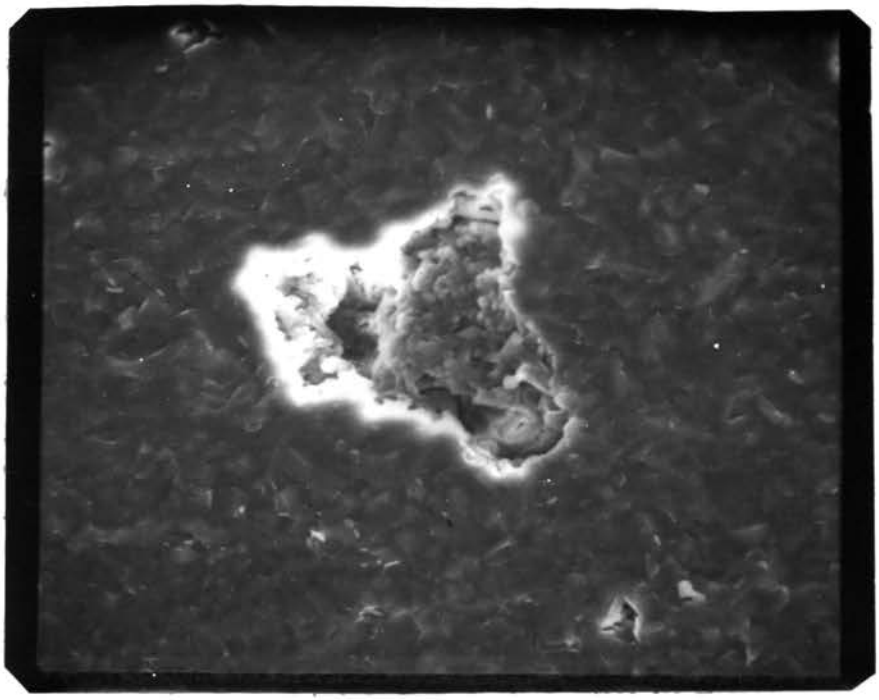

a) 500X

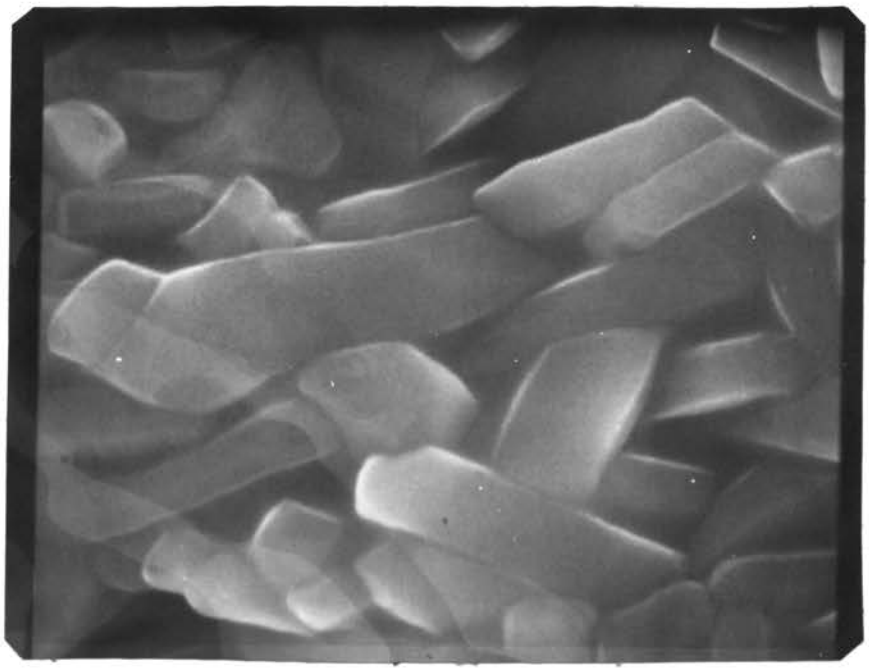

b) 5000X

Figure 8: MULLITE FRACTURE SURFACE

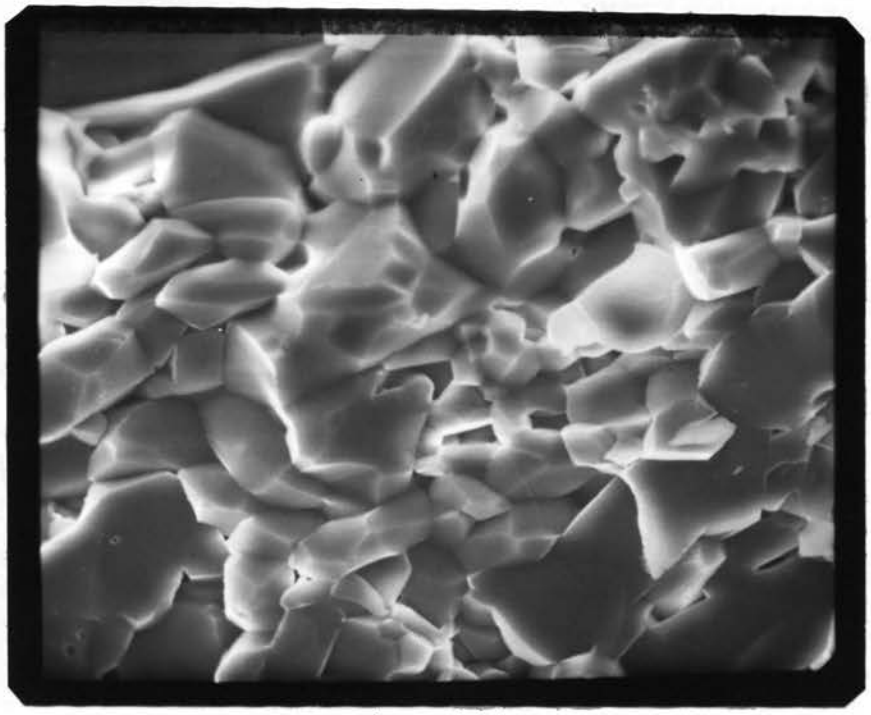

a) 1000X

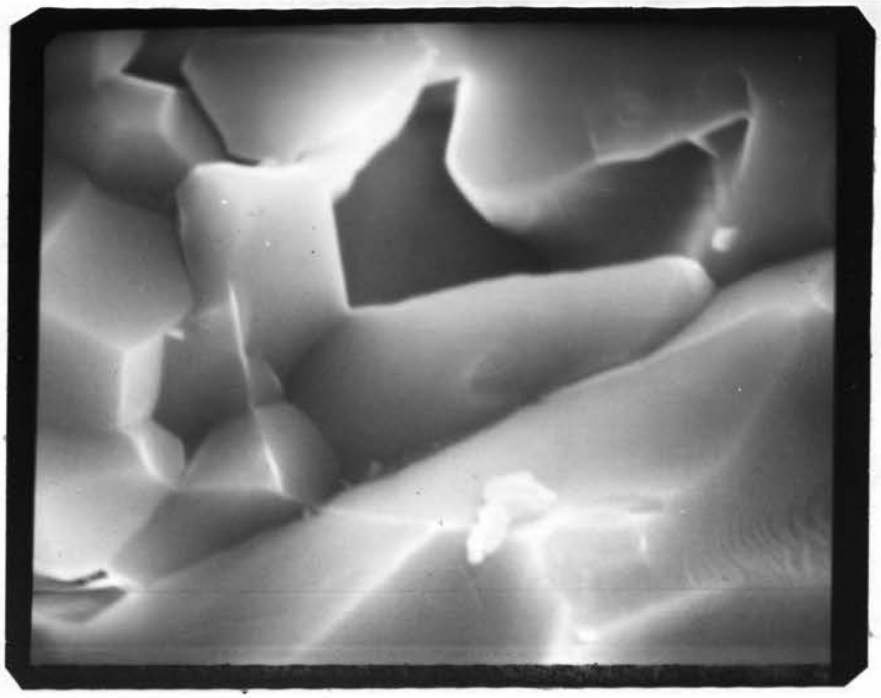

b) 5000X

Figure 9: ALUMINA (99.5% dense) FRACTURE SURFACE

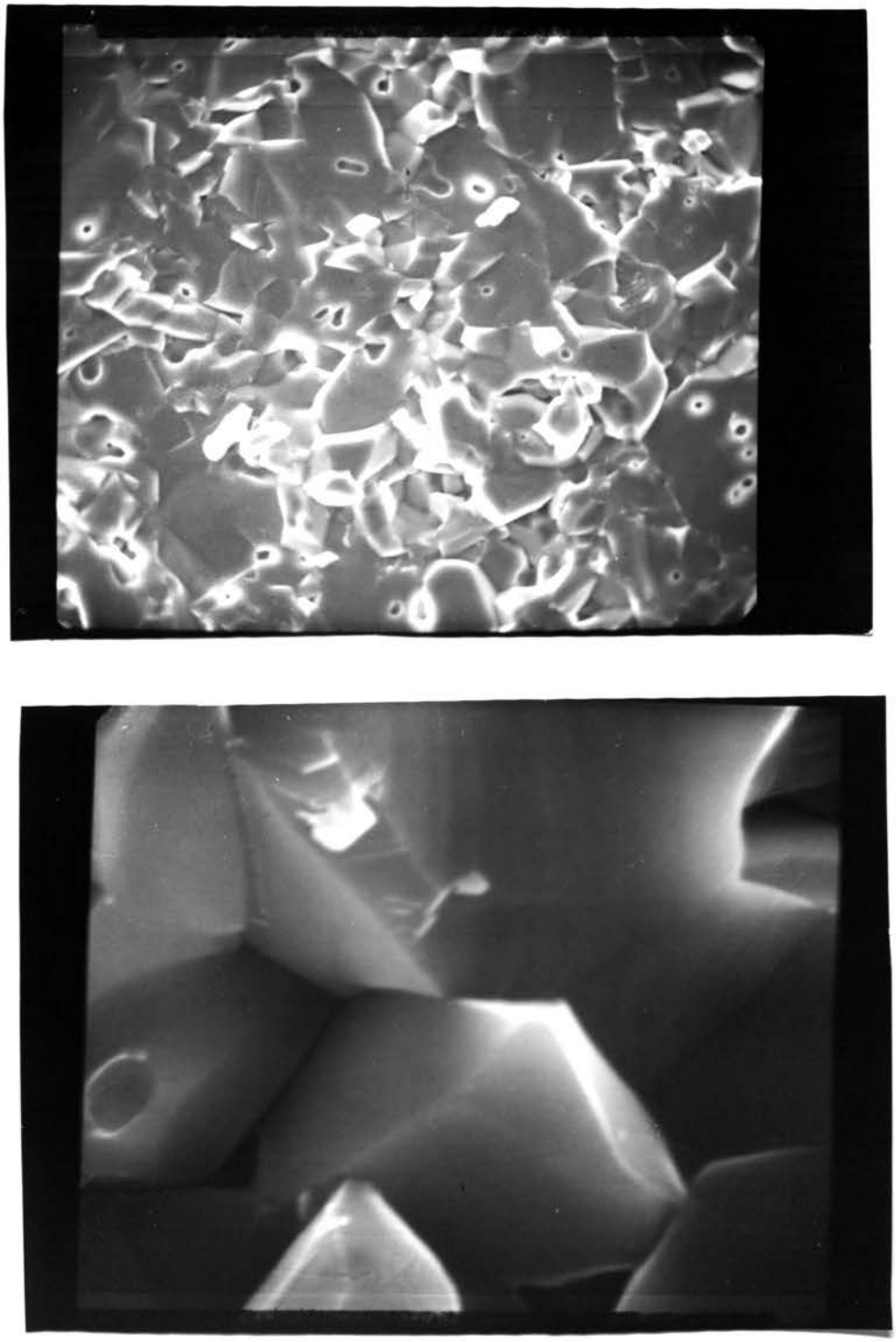

Figure 10: ALUMINA (99% dense) FRACTURE SURFACE

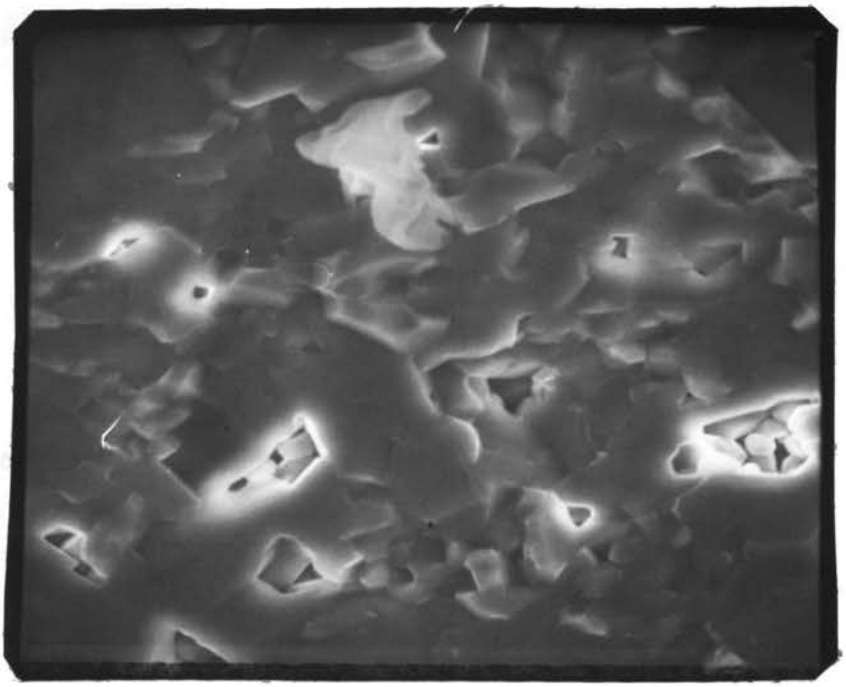

a) 1000X

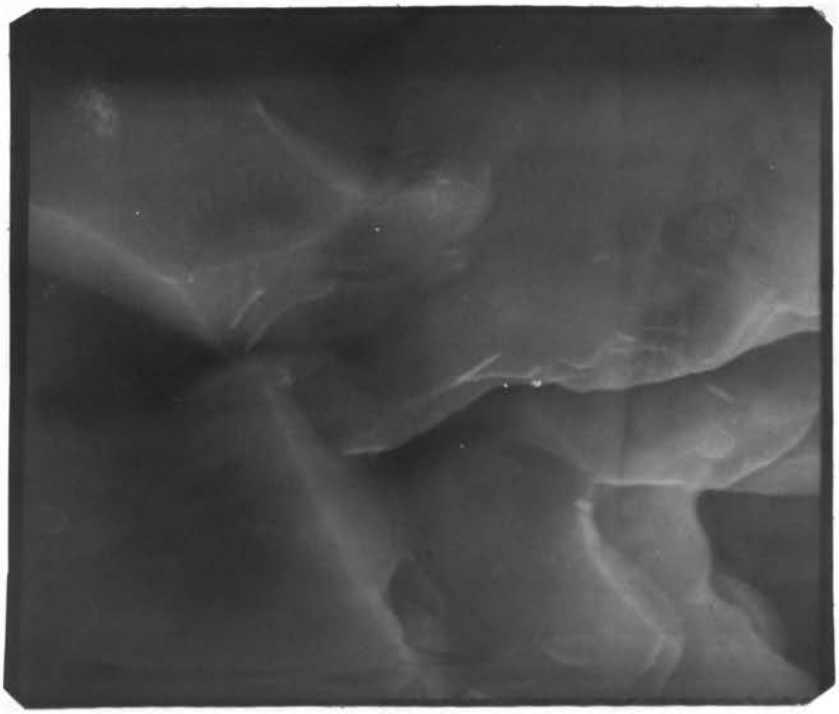

b) 5000X

Figure 11: ALUMINA (96% dense) FRACTURE SURFACE

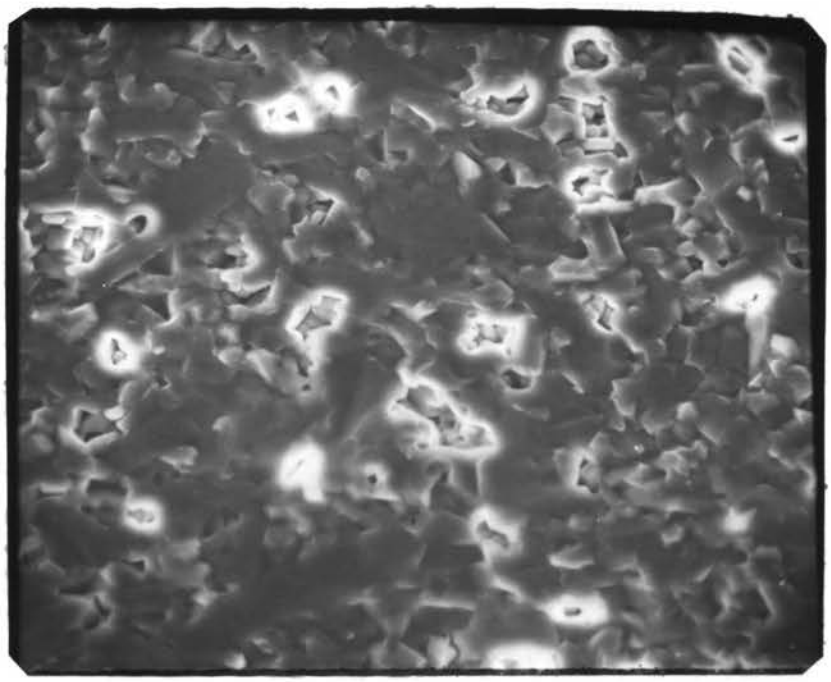

a) 500X

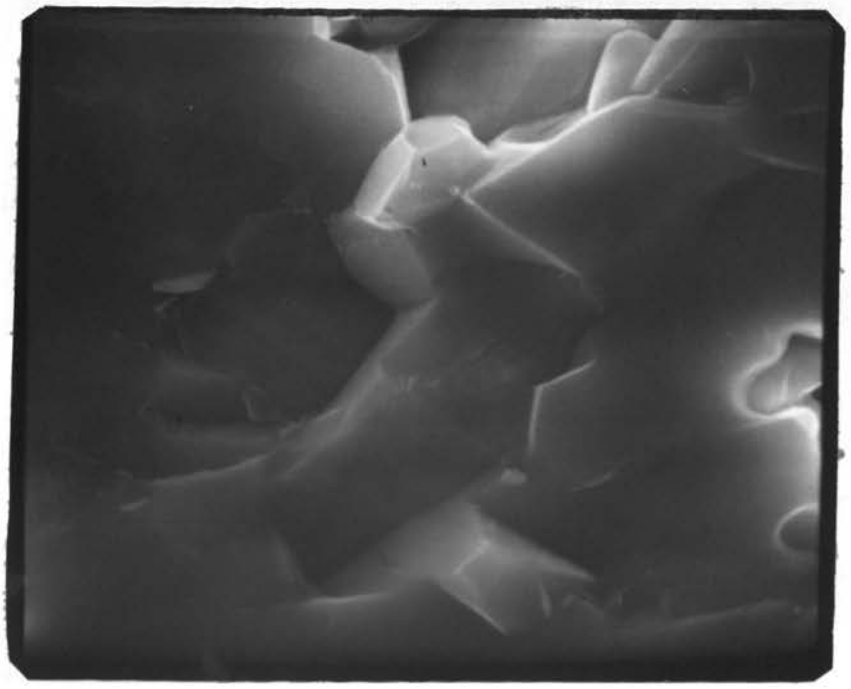

b) 3000X

Figure 12: ALUMINA (94% dense) FRACTURE SURFACE

V. DISCUSSION OF RESULTS

After the extensive study and experimentation of Summers,[3] the author was convinced that Summers' method of fracture surface energy determination would prove the most reliable in calculating values in the present work. The general form of Srawley's[4] surface energy equation comes about through simple mechanics and the definition of surface energy itself. If the unnotched portion of the specimen (Fig. 2) is considered to act as a simple beam when loaded in 3-point bending, the stress (σ), at the crack tip will be given by:

$$\sigma = \frac{My}{I} \tag{7}$$

Here $M = p_m L/4$ and y is assumed to be $(d-c)/2$. The moment of inertia (I) is assumed to be $b(d-c)^3/12$, which results in:

$$\sigma = \frac{3pL}{2b(d-c)^2} \tag{8}$$

If this value of is then substituted into Griffith's equation, $[\gamma = \frac{\pi\sigma^2}{2E}]$, we find:[3]

$$\gamma = \frac{9\pi p^2 L^2 c}{8Eb^2(d-c)^4} \tag{9}$$

This gives us the basic form of our Eq. (6). The variables and other constants introduced by the

experimentation of Srawley are quite involved and are dealt with quite thoroughly in Ref. 4.

Rose and English[5] found that for geometrically similar beams, $\frac{p^2}{d^3}$ must equal a constant if the Griffith criteria is to hold. As we examine our final choice of a surface energy equation, we see that if:

$$\gamma = \frac{9p^2\pi L^2 c}{8Eb^2d^4}\left[A_o+A_1\left(\frac{c}{d}\right)+A_2\left(\frac{c}{d}\right)^2+A_3\left(\frac{c}{d}\right)^3+A_4\left(\frac{c}{d}\right)^4\right]^2$$

when L/d, c/d and L/b are held constant, Srawley's equation reduces to p^2/d^3 (constant), and therefore satisfies Rose and English's criteria.

Summers* found that the shape of the crack tip had no great effect on the surface energy values obtained from the Srawley equation and that in plexiglas the most consistent data resulted from samples having a $(\frac{c}{d})$ ratio of ≈ 0.3, but that this was not mandatory. He also found that Griffith's theory for microscopic cracks holds true for notch widths as wide as 0.08". Since the width of our notches was between 0.01 and 0.03" we were well within the "limits" set by Summers.[5]

---

* SUMMERS, D. A. (1970), Personal Communication

The deviation of the surface energy values of all the aluminas, the steatite and the mullite specimens was on the order of 10%, while the deviation of the individual values for the zircon was almost 30%. One reason offered for the increased variation with the zircon is that it was impossible to apply the load to the zircon specimens at a slow enough rate to cause complete fracture of the specimen without breaking it in two. With the other materials, several specimens were broken that remained stationary and did not fall from their loading supports when fracture occurred. When the knife edge was lowered further on a specimen that broke but did not fall into two halves, no load whatsoever was indicated by the recorder to cause the halves to separate. Since the recorder-load cell combination was accurate to 0.01 pounds, it was felt that very little excess energy was used in the fracture of those specimens that broke but did not fall from the loading supports.

One reason that the low value of fracture surface energy for the zircon was not too surprising was that all 21 specimens were notched with the same wire blade, while some of the other materials (i.e. alumina) required 2 to 3 blades to notch just one specimen. The great irregularity in particle size (Fig. 6) helps account for the large variance in the value of γ. Since in some instances large crystals were fractured rather than the fracture

path following the grain boundaries, this could also cause a variance of the γ values, depending upon the size of grains present on each fracture surface. This reasoning is partially based on the facts given by Swanson,** who stated:

> "Thermodynamic free surface energy, as measured by liquid drop methods, is lower than the cleavage surface energy along a specific crystalline plane in an actual single crystal. The single crystal cleavage surface energy is again lower than that for fracturing a polycrystalline ceramic piece. And for polycrystalline ceramics, the fracture surface energy definitely has different numerical values for different grain sizes."

From viewing the photomicrographs of the aluminas, one sees that as the densities increase the particle size increases and the grains appear to become more distinct. (See Figs. 9-12. The 94 and 96% aluminas contain several regions where the grain structure is not as clearly defined as in the 99 and 99.5% aluminas.) Since there is such a difference in the fracture surface energy values for the 99 and 99.5% aluminas, it would be interesting to measure the γ values for Coors 94 and 96% aluminas to see if there is a definite trend in the surface energy of these materials in comparison with the data already collected.

** SWANSON, G. (1970), Personal Communication

The fracture in the aluminas seems to have been almost entirely along the grain boundaries. The interwoven crystalline network of the mullite caused fracture to occur through many of the grains, rather than along a grain boundary. This intergranular fracture may be one reason for the low value of γ for mullite. Because of the intergranular fracture, a clear view of the crystalline network of the mullite was possible only by looking into a pore which was not directly on the fracture surface. (See Fig. 8)

The steatite, although somewhat more porous than any of the other materials, still had a much higher γ value than the mullite and zircon. Figure 23 shows that the steatite's fracture surface was slightly more irregular than the other materials and this could mean that much more new surface was created than accounted for. This would help justify that our value may be somewhat high.

Noting paired values for ΔT and the fracture surface energy values, (Table I), one can readily see that there is no direct relationship between the maximum thermal shock (ΔT) the material can withstand before cracking begins and the fracture surface energy. This is not surprising and would almost be expected since thermal shock or the resistance to thermal shock is not solely a function of surface energy. Once a crack has been initiated in a

material from thermal shock the fracture surface energy value becomes much more important and surely has much to do with the depth of penetration of the crack. There are at least three other material properties which are quite important when discussing thermal shock. These are: Young's modulus, thermal conductivity and the thermal expansion coefficient. One might speculate that one reason the mullite showed such a good thermal shock resistance was that it combines a low E modulus with a high tensile strength and a low coefficient of thermal expansion. The interwoven crystal structure may also help by strengthening the network and possibly allowing a slight internal movement to help relieve some of the stresses and thus postpone failure.

VI. CONCLUSIONS

In order to be more confident in the fracture surface energy values obtained in this work, an effort should be made to determine the error involved when it was assumed that the newly created surface was a perfectly smooth plane. The existing values for γ could then be divided by this "factor" and one would have a more accurate value.

The main purpose of the measurements of γ in this work was to obtain a fairly valid fracture surface energy value to use in the thermal shock investigation mentioned in the introduction. At present it is not known if the fracture surface energy values measured on these materials are a representative for all similar materials. Since density and grain size are so important, these would have to be specified with the γ value. What is important here is that the γ values are representative of the materials used in the thermal shock study. Since the γ measurements were made on a random selection of the thermal shock specimens, one should be quite confident in their accuracy.

In his discussion of polycrystalline ceramics, Weiderhorn[13] explains that the fracture surface energy values for polycrystalline ceramics are an order of magnitude higher than the fracture surface energy values for single crystals of the same material. This is because

in polycrystalline materials, cracks must extend through and around several grains and that while traveling along grain boundaries many "high energy obstacles" may be encountered. From his work he concluded that (in agreement with Swanson, and others) there definitely is a relation between the fracture surface energy values for the same material with different grain sizes; Weiderhorn's conclusion being that the fracture surface energy increased with increasing grain size. The writer has no definite data which would prove or disprove this statement, but feels that the trend should be toward higher values with decreasing grain size. The reasoning for this is merely the fact that since smaller particles have much more grain boundary area, upon fracture one is bound to encounter more "high energy obstacles[13]" with smaller-grained materials than in polycrystalline materials with larger grains. It must be remembered too, that sintering and grain growth take place in order to lower the internal energy of the system.[6] This should all then imply that it should require less energy to fracture a material with larger grains.

The value of fracture surface energy for a material should be important in the prediction of fracture resistance of solids. However, before these values can be of any great help to people, it will be necessary to develop a standard formula for the γ calculations. This formula must be valid for a wide range of variations of the specimens being tested. Summers[3] has shown the

possibility of getting a broad spread of values for exactly the same material when some of the "accepted" surface energy equations were used. For this reason one should thoroughly examine not only the method used for the breaking of the specimens, but also note the range of validity of the equation used in the final calculations. If this is not done, some very false conclusions may result from data that is not really "legitimate."

Although Summers' work also showed that there was no great variation in results by using different crack shapes and widths (within limits), it is felt that increasing the sharpness or at least reducing the width of the crack as much as possible might help to reduce any stored or "extra" energy input while loading the specimen.

One final suggestion or word of caution: one must always be aware of the loading rate at which the specimens are broken. Faster loading rates result in fracture at reduced loads. To obtain more consistent data, it would be advisable to have a loading set-up that would insure a constant loading rate for all specimens.

VII. APPENDICES

APPENDIX A

SURFACE ENERGY SPECIMEN PREPARATION

A-1. Cutting of rectangular specimen from rods:

The 6-inch rods of each material were first cut into 3-inch lengths. This was necessary because the diamond saw used to cut the specimen could be raised less than 4 inches about the top of the sample holding vise. (See Fig. 13 for picture of saw.) A holder for the rods was constructed from two blocks of aluminum. These each had a cylindrical channel cut through them so that when placed together they would form a hole of ½" diameter. (Fig. 14) The holder was then placed in the jaws of the diamond saw so as to hold the 3-inch rod in a rigid vertical position. By use of a T-square the specimen was aligned perpendicular to the blade. It was noted that merely having the specimen perpendicular to the base of the vise did not result in the specimen and blade being at right angles. After the rod was correctly positioned, two parallel sides of the rod were sliced off (Fig. 15). The rod was then rotated 90° and successive slices were made through it. Extreme care must be taken when cutting the rods, especially specimens of harder materials such as alumina. A constant stream of coolant must be flowing on the blade and specimen during the entire operation. The speed of travel of the blade through the specimen is most critical. If the rate is too fast, overheating of both the blade and the specimen will occur and this is injurious to both. Excessive speed also causes vibration in the rod and may cause thin specimens to break.

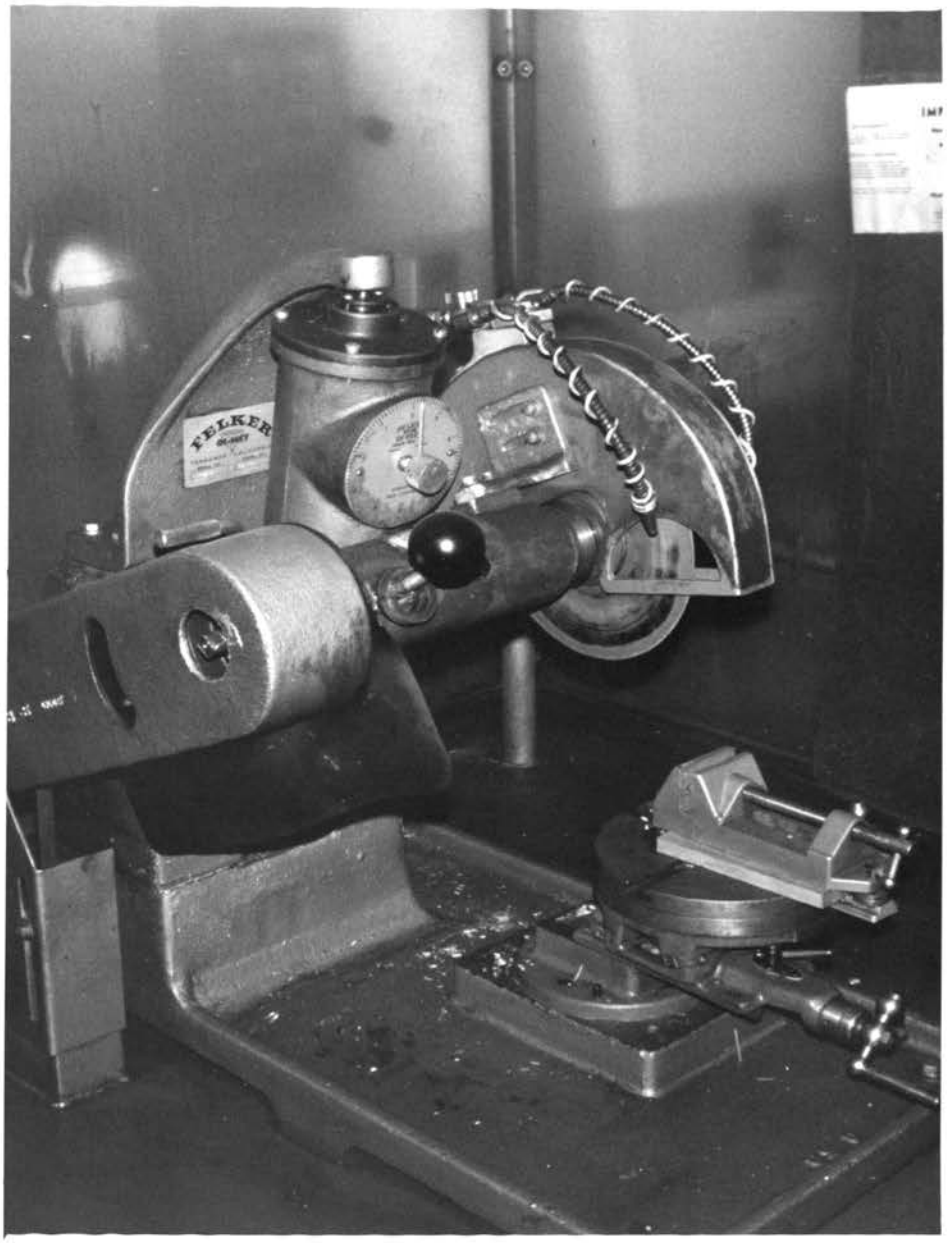

Figure 13: THE DIAMOND SAW

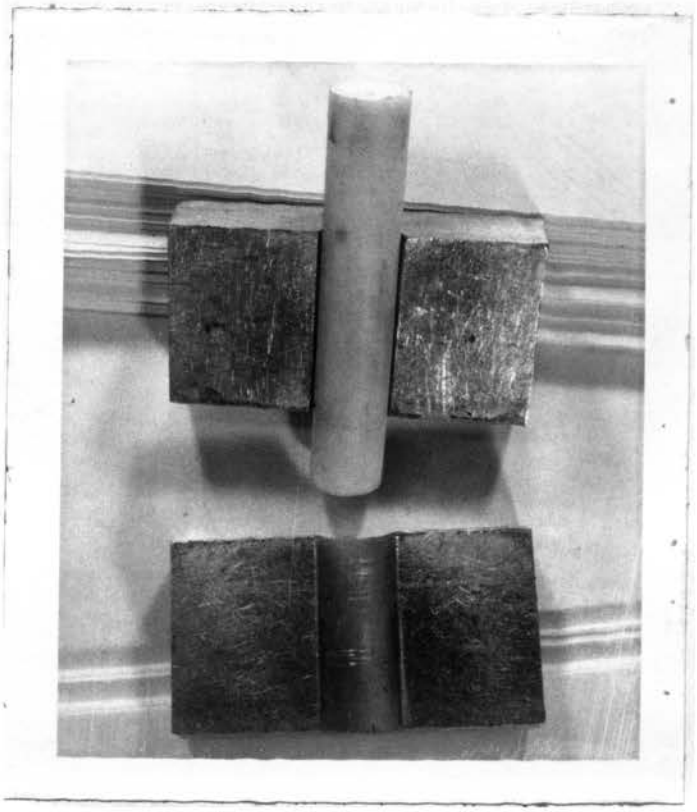

Figure 14: THE SPECIMEN HOLDER

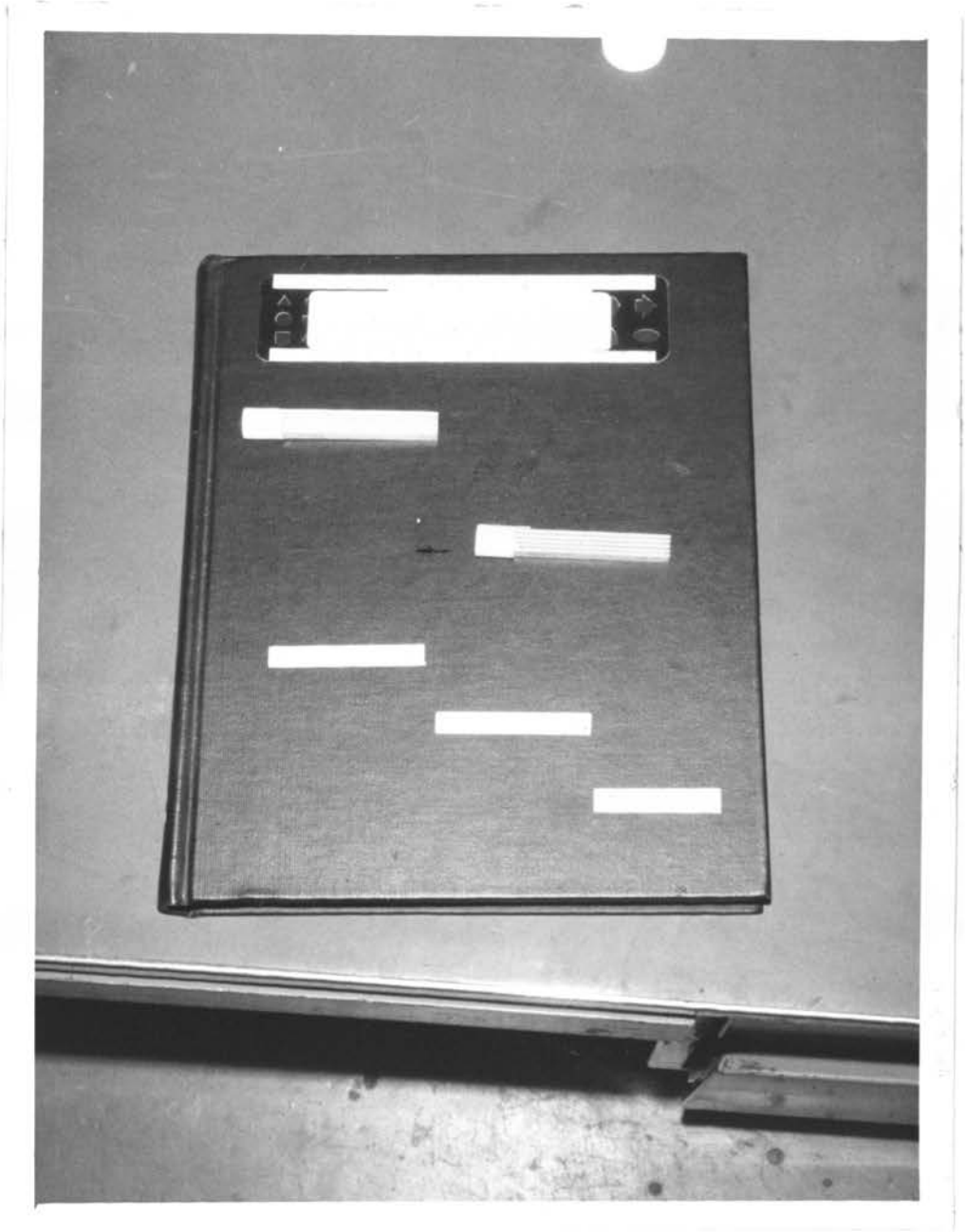

Figure 15: FINISHED SPECIMENS

The thickness of the specimen may be determined by noticing the travel on the vernier scale of the diamond saw base or merely by eye. The minimum thickness that can be cut is dependent not only on the operator of the saw but also on the material being cut. In any case, a thinner specimen may always be cut at lower speeds, (speed here implying the rate of drop of the blade into the rod.)

A-2. Notching the surface energy specimen:

Two methods were used to notch the rectangular surface energy specimens; (1) with a wire saw and (2) by using a diamond saw. In either case it was necessary to mark the center of the specimen before making the cut. It was found that one could mark them quickly and more accurately by cutting a thin piece of paper in the same length as the specimen and folding it exactly in half. The folded paper was then opened and the sharp outside edge of the fold used as an indicator of the specimen's center. By placing this paper over the specimen, the center line could then be marked with the sharp point of a hard lead pencil.

(1) The wire saw:

The wire saw is the piece of apparatus pictured in Fig. 17. Wires of varying diameter may be purchased, ranging from as small as 0.0035". Some blades are

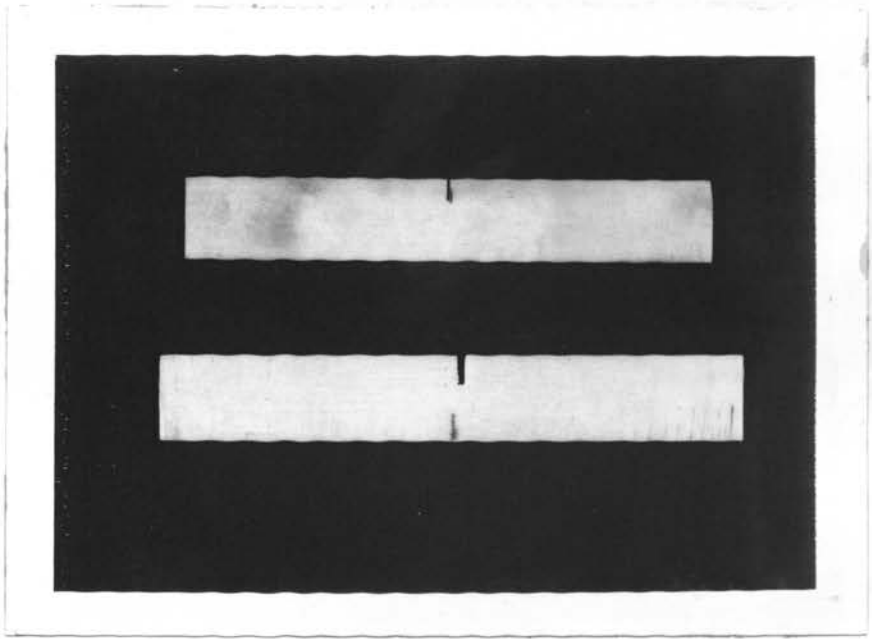

Figure 16: NOTCHED SPECIMENS: (top) wire saw cut, (bottom) diamond blade cut

available which have diamonds impregnated in them. We found these to be most unsatisfactory. Most of these "blades" are merely continuous wire loops which carry an abrasive compound (in our case 600 mesh boron carbide). The contents of the cutting mixture we used was: 1 part water, 1 part boron carbide and 4 parts glycerine (by weight). This mixture has a tendency to separate upon sitting and should be mixed vigorously before each using.

The main difficulty with the wire saw notching is simply that the blades are quite costly and their life span was usually quite short. Some "hints" which will aid one in the use of the wire saw will be given though, since it is a very effective method of producing a very thin cut in a material.

It was found that the width of the resulting crack was effectively the diameter of the blade that was used to make the cut. With much patience and a good supply of blades, a cut can be made in most any material providing that the specimen is not thick enough to keep the liquid abrasive from penetrating the entire length of the crevice.

"HINTS"

(a) First of all, don't be in a hurry to make a cut. The time necessary to make a cut 0.100" deep in a hard

Figure 17: THE WIRE SAW

material (i.e. alumina) that is .025 - .035" thick, may range from 3 to 15 minutes. If one has a very good blade, it may be possible to make the cuts in a minimum time. The main problem causing blade breakage is that the spot where the wire is welded together tends to be of a larger diameter than the rest of the blade and this does not allow the wire to run smoothly over the specimen.

(b) Be sure to mark the center of the specimen before placing it in the saw. In order to be able to easily determine the advance of the wire through the material, it was found that a piece of cellophane tape placed horizontally on the specimen at the depth the notch is desired to stop, makes it much easier to determine when the notch is deep enough. The reason the depth of penetration of the wire is hard to observe without the tape is that the black cutting compound tends to coat the center of the sample and hide the pencil-marked crack depth. If the tape extends a small distance from the area being cut, the tape's top edge is easily visible and the wire's depth readily observed.

(c) Before beginning to cut the specimen with the wire saw, it helps if one will very carefully place a layer of cellophase tape along the back side of the sample holder. This tape should be positioned so that its top edge is located where the bottom edge of the specimen will sit. Then, when the specimens are put in the holder, they may

be slid in until they are firmly resting on the top edge of this tape and if the specimen is then perfectly uniform in height, every specimen will be cut straight and little effort is necessary to align them.

(d) If another piece of tape is stuck to the back side of the sample holder (can be seen by closely examining Fig. 17) this will create a small pocket between the tape and the sample. This pocket serves as a reservoir for the cutting fluid and if kept full at all times, it will aid in the cutting.

(2) The diamond saw:

Notching was done with the diamond saw when it became quite costly to notch the specimens with the wire saw. Using this method it is possible to notch several specimens at the same time. The general idea of this method is that the specimens are embedded in a medium and then a thin diamond blade is passed through the entire block which contains them. In this work sealing wax was used to embed the specimens. A piece of wood with several parallel cuts in it was used to hold the specimens vertical while the hot sealing wax was being poured into a rectangular mould. It was first necessary to allign the centers of the specimens and make sure that they were all flat against the bottom of the mould. The wax was then poured into the mould and

everything but the notched wood block was covered with wax. After the wax had hardened the sides of the mould were removed and the piece of wood pried off. The block of wax was then placed in the mould again and the remaining portion filled with wax; the end result being a rectangular block of sealing wax with several samples "hidden" inside. (Figures 18 and 19 show the two steps mentioned above.) With the blade of the diamond saw set at a constant depth, the sample block was mounted under the blade and moved into it. (The entire sample block must be level or else the notch depth will not be predictable.) In this work a blade thickness of 0.012" was used. This resulted in a notch width ranging from .028 - .030". It might also be advisable to mention that the use of some type of mould release is advisable when moulding sealing wax, as it has a tendency to adhere to most any uncoated surface.

To remove the notched samples from the wax, they were soaked in an acetone bath. Boiling water would have melted the wax, but it was feared that differences in expansion coefficients of the specimen and the wax might result in breaking the specimen inside. Methanol will also dissolve the wax, but more slowly. It was used in the final cleaning of the specimens.

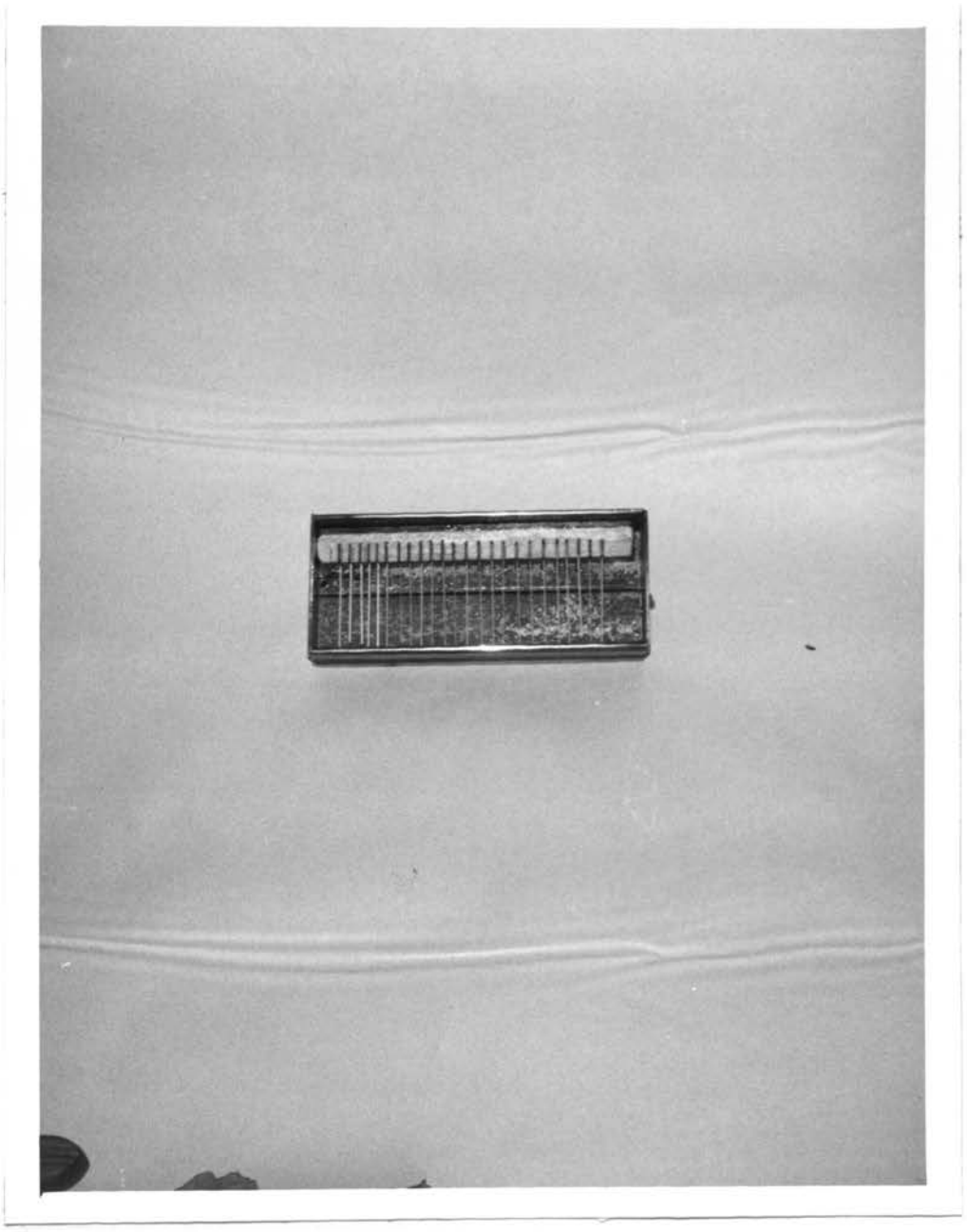

Figure 18: EMBEDDING SPECIMENS: Step I

Figure 19: EMBEDDING SPECIMENS: Step II

A-3. Breaking specimens:

The unit used to break the surface energy samples is pictured in Fig. 1. The knife edge was centered over the inverted crack in the specimen and the load applied by slowly rotating the small gear on top the jig. This small gear drove the large center gear which in turn forced the shaft downward. Directly above and connected to the knife edge is a small Kistler, model 912 quartz load cell. This unit contains a pressure sensitive quartz crystal. When a load is applied to it a charge is produced which is directly proportional to the load applied. The load cell was sensitive to loads ranging from 0.01 to 5,000 psi. It was coated with a 3140 RTV coating to insulate it from any possible heat that might be absorbed from the operator's hands. A calibration of our load cell (pressure vs. output) may be found in Fig. 21. The output of the load cell was sent through a charge amplifier which contained a calibration device that allowed us to adjust the amplifier to match the output of our load cell. The output of this amplifier then fed into our recorder and the load could be read directly from the recorder paper in pounds per square inch. This load (p), was then used in the surface energy equation, Eq. 6. Figure 20 shows the entire experimental set-up.

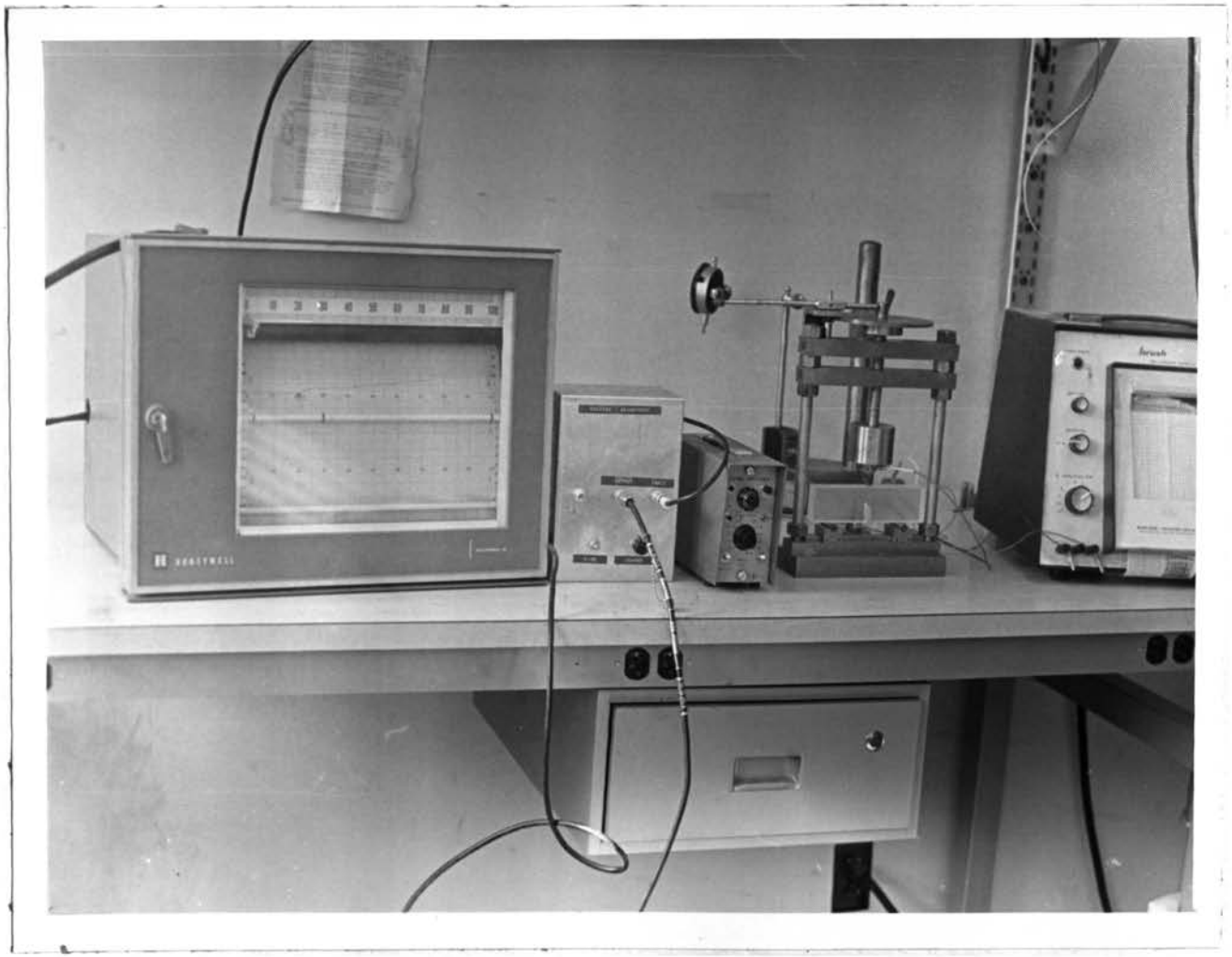

Figure 20: THE EXPERIMENTAL SET-UP

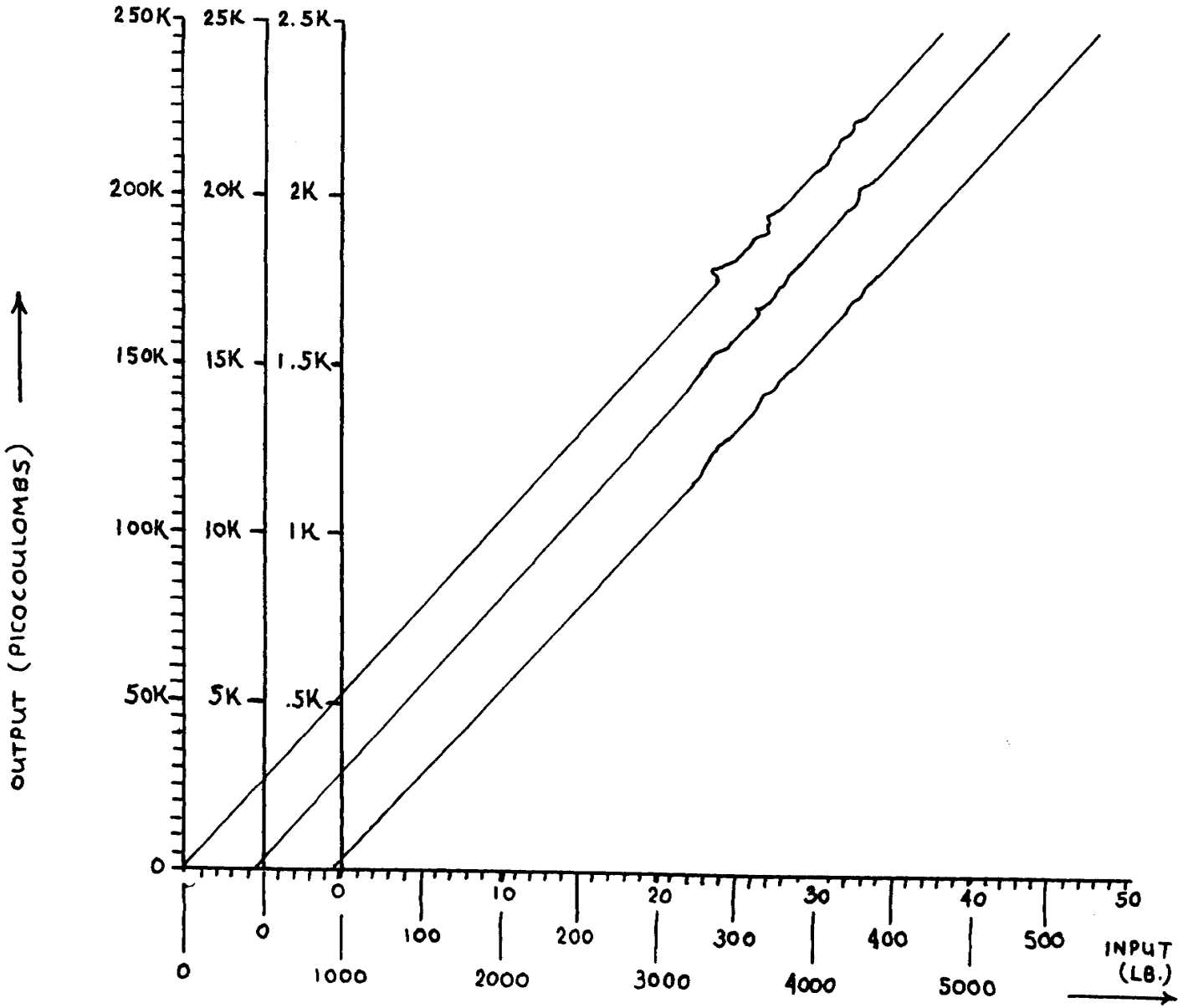

Figure 21: LOAD CELL CALIBRATION

APPENDIX B

FRACTURE EDGE OF SPECIMENS

B-1. Profile of Fracture Edge:

Figures 22 through 28 show the fracture edge of the broken specimens. The photos are of all seven different materials used and are magnified 16 to 24 times actual size.

The purpose in taking these photos was to examine the fracture edge and see just how irregular it was. All the calculations of fracture surface energy (γ) assume the fracture surface to be perfectly smooth. From the photos seen earlier of the magnified surface, one can readily see that in many cases fracture occurred almost entirely along grain boundaries. This means that the surface was surely not smooth and that this will cause the reported values of γ to be slightly high, the magnitude of error depending upon the individual specimen's grain size.

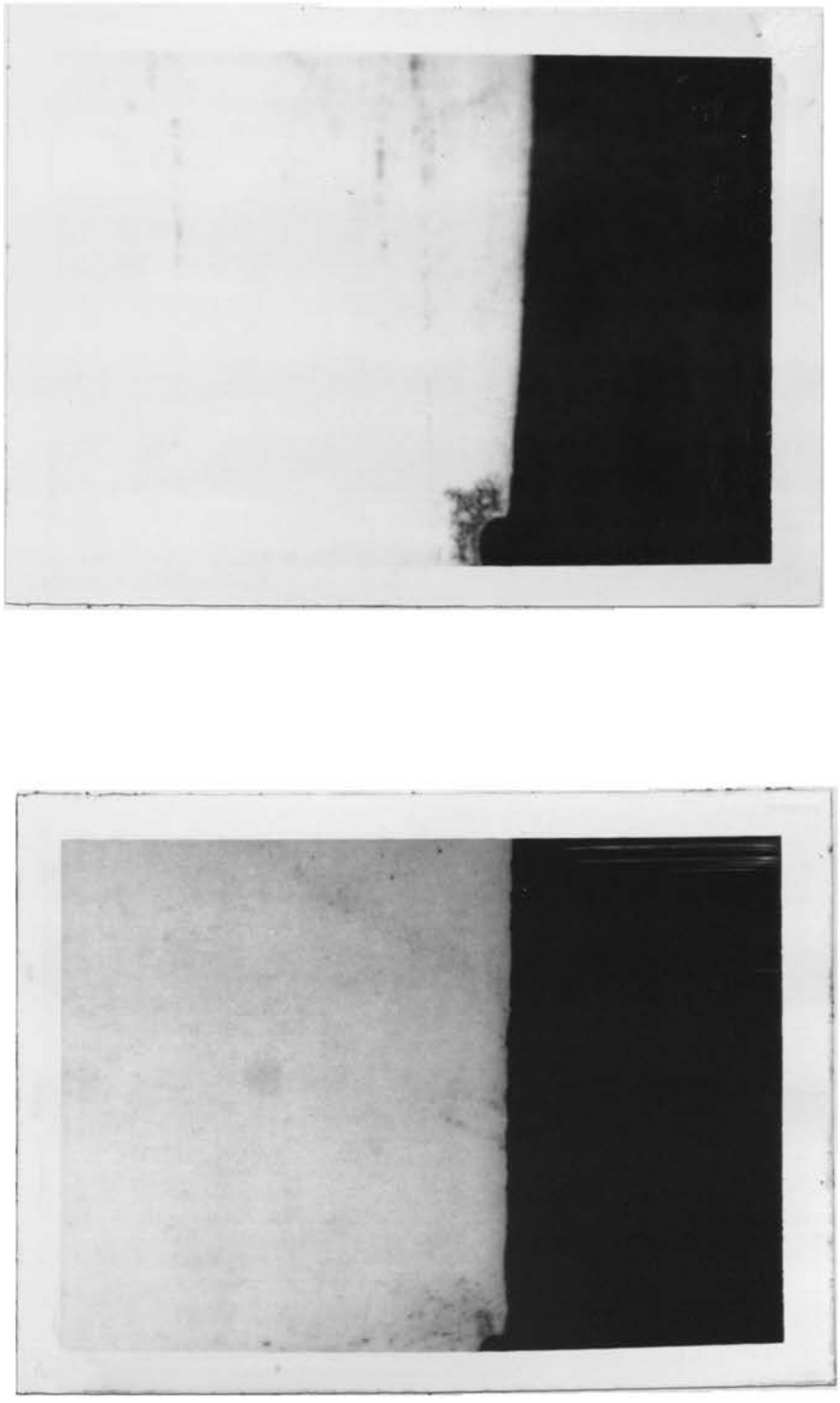

Figure 23: STEATITE FRACTURE EDGE

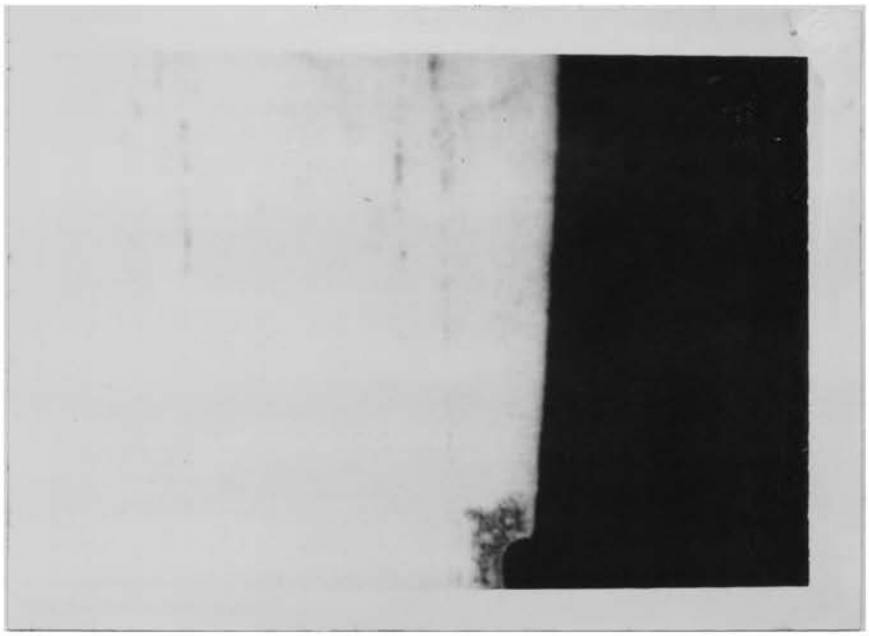

Figure 22: ZIRCON FRACTURE EDGE

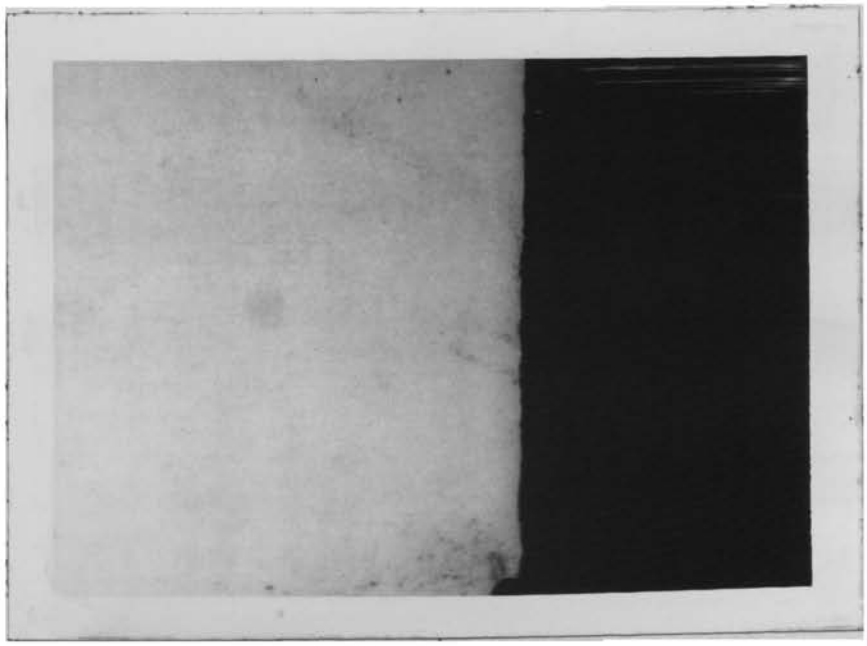

Figure 23: STEATITE FRACTURE EDGE

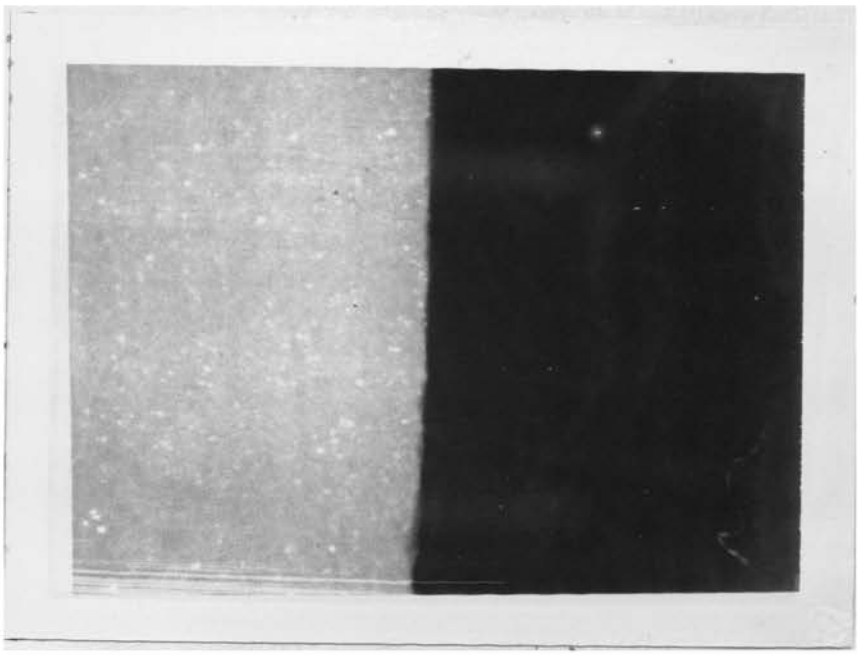

Figure 24: ALUMINA (99.5% dense) FRACTURE EDGE

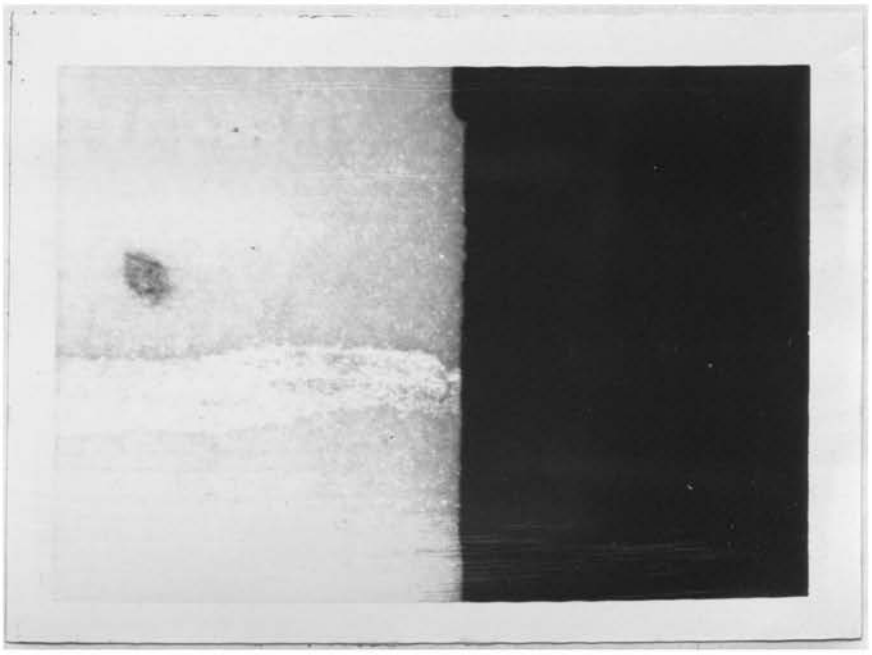

Figure 25: ALUMINA (99% dense) FRACTURE EDGE

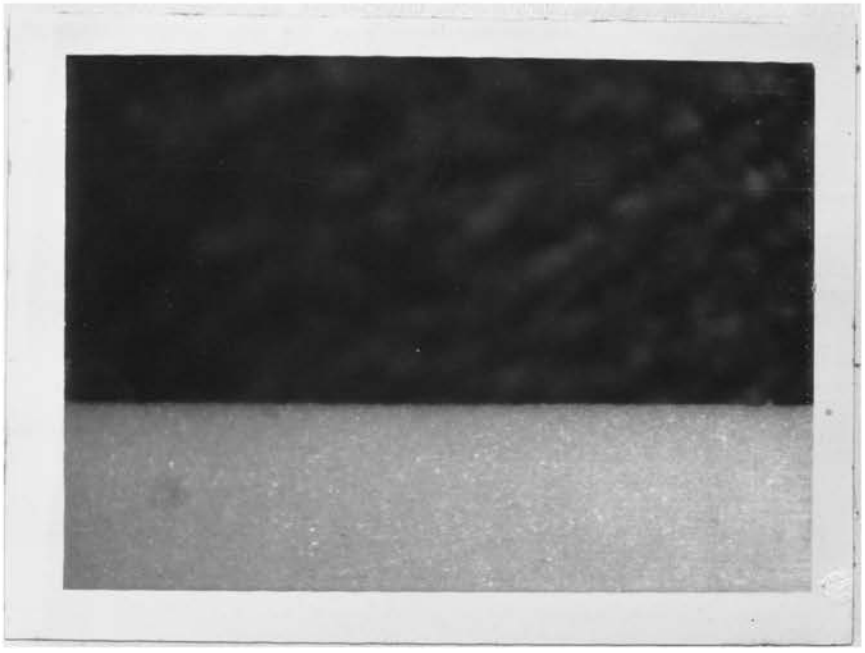

Figure 26: ALUMINA (96% dense) FRACTURE EDGE

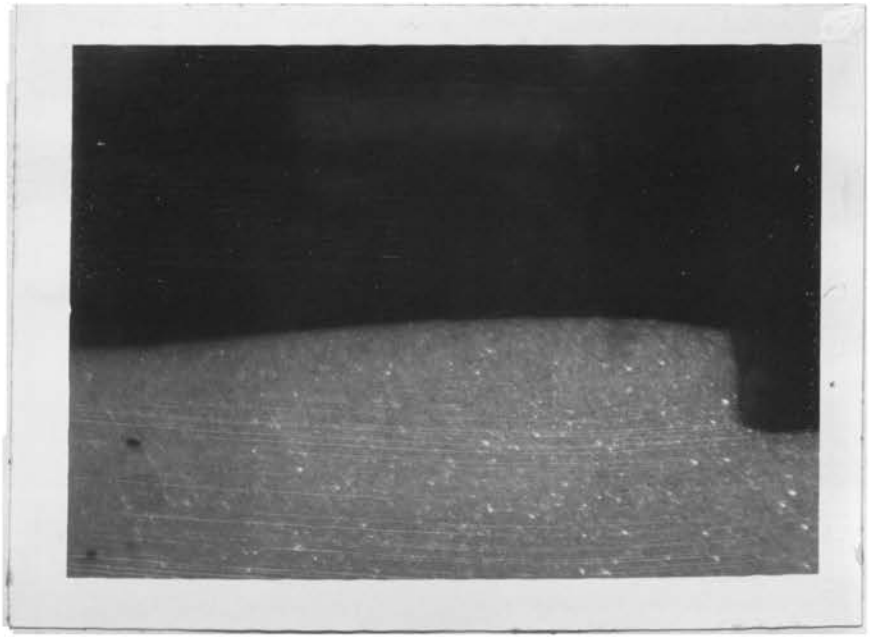

Figure 27: ALUMINA (94% dense) FRACTURE EDGE

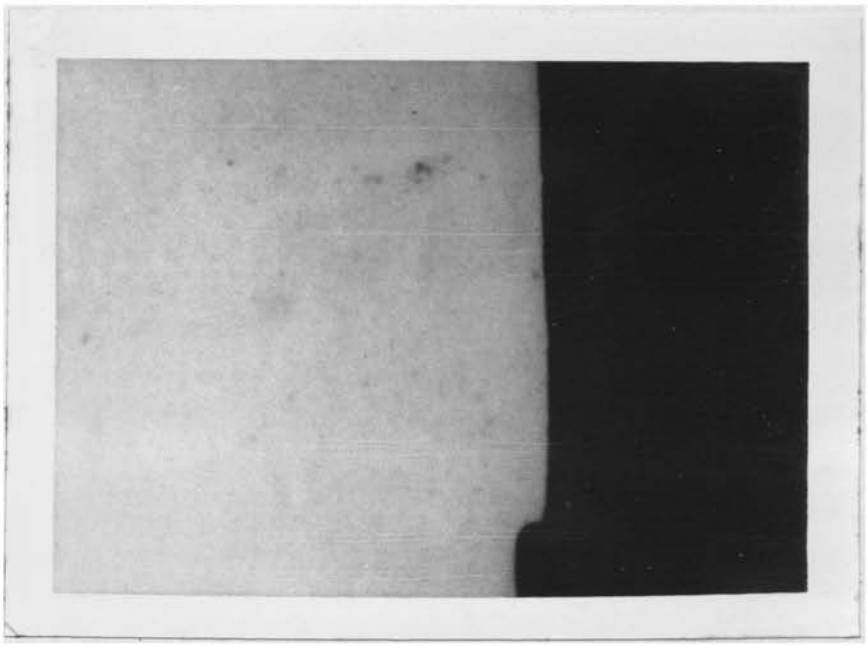

Figure 28: MULLITE FRACTURE EDGE

APPENDIX C

DATA FROM SURFACE ENERGY SPECIMENS

STEATITE #460

Sample Number	L	d	b	c	c/d	p	ρ	Fracture Surface Energy
c-1(1)	1.81"	0.348"	0.034"	0.107"	.3075	4.94#	2.63	23,871 ergs/cm^2
c-1(3)	1.81	0.350	0.036	0.101	.2886	5.16	2.63	20,718
c-1(5)	1.81	0.349	0.049	0.099	.2837	6.24	2.63	16,090
c-1(6)	1.81	0.354	0.042	0.119	.3362	5.26	2.63	19,484
c-1(7)	1.81	0.346	0.040	0.088	.2543	6.38	2.63	22,281
c-2(1)	1.81	0.352	0.043	0.123	.3494	5.17	2.63	19,575
c-2(2)	1.81	0.352	0.030	0.094	.2670	4.39	2.63	18,992
c-2(3)	1.81	0.350	0.028	0.105	.3000	3.61	2.63	17,772
c-2(4)	1.81	0.354	0.053	0.100	.2825	6.60	2.63	14,632
c-2(5)	1.81	0.365	0.031	0.096	.2630	5.34	2.63	23,029
c-2(7)	1.81	0.360	0.045	0.096	.2667	6.74	2.63	18,519
c-2(8)	1.81	0.361	0.045	0.094	.2604	6.48	2.63	16,428
c-3(1)	1.81	0.362	0.032	0.113	.3122	4.76	2.63	22,673
c-3(2)	1.81	0.364	0.034	0.088	.2418	6.42	2.63	24,972

STEATITE #460 (cont.)

Sample Number	L	d	b	c	c/d	p	ρ	Fracture Surface Energy
c-3(3)	1.81"	0.362"	0.044"	0.116"	.3204	5.90#	2.63	19,223 ergs/cm^2
c-3(4)	1.81	0.363	0.036	0.105	.2893	6.10	2.63	25,945
c-3(5)	1.81	0.360	0.031	0.105	.2917	4.62	2.63	20,850
c-3(7)	1.81	0.352	0.030	0.112	.3182	4.16	2.63	22,167

(Crack width for all specimens = 0.010")

ZIRCON (ALSIMAG #475)

Sample Number	L	d	b	c	c/d	p	ρ	Fracture Surface Energy
2-(D-2)	1.81"	0.353"	0.036"	0.090"	.2550	5.34#	3.67	11,034 ergs/cm^2
3-(D-2)	1.81	0.353	0.026	0.104	.2946	3.36	3.67	11,796
4-(D-2)	1.81	0.354	0.038	0.106	.2994	6.86	3.67	20,372
5-(D-2)	1.81	0.307	0.028	0.095	.3094	3.08	3.67	12,401
6-(D-2)	1.81	0.308	0.037	0.085	.2760	4.74	3.67	14,029
7-(D-2)	1.81	0.308+	0.040	0.080	.2597	5.24	3.67	13,489
8-(D-2)	1.81	0.308	0.060	0.064	.2078	8.50	3.67	11,941
9-(D-3)	1.81	0.397	0.051	0.103	.2594	9.34	3.67	11,963
10-(D-3)	1.81	0.395	0.031	0.126	.3190	4.54	3.67	10,551
11-(D-3)	1.81	0.395+	0.051	0.118	.2987	7.84	3.67	10,480
12-(D-3)	1.81	0.366	0.055	0.099	.2075	10.16	3.67	16,580
13-(D-3)	1.81	0.364	0.046	0.068	.1868	8.74	3.67	14,081
14-(D-3)	1.81	0.364	0.032	0.112	.3077	4.88	3.67	13,909
15-(D-3)	1.81	0.363	0.027	0.088	.2424	4.39	3.67	11,383

ZIRCON (cont.)

Sample Number	L	d	b	c	c/d	p	ρ	Fracture Surface Energy
18-(D-1)	1.81"	0.356"	0.039"	0.096"	.2697	6.20#	3.67	13,324 ergs/cm^2
19-(D-1)	1.81	0.339	0.039	0.100	.2950	4.44	3.67	9,060
20-(D-1)	1.81	0.360	0.056	0.070	.1944	12.20	3.67	16,123
21-(D-1)	1.81	0.362	0.045	0.092	.2540	8.82	3.67	17,742

(Crack width for all specimens = 0.010")

MULLITE (MV-30)

Sample Number	L	d	b	c	c/d	p	ρ	Fracture Surface Energy
G-1(1)	1.81"	0.371"	0.034"	0.107"	.2884	4.80#	2.83	11,328 ergs/cm^2
G-1(2)	1.81	0.375	0.036	0.102	.2720	7.20	2.83	20,391
G-1(4)	1.81	0.376	0.036	0.102	.2713	4.25	2.83	7,020
G-1(5)	1.81	0.367	0.033	0.101	.2752	5.95	2.83	18,013
G-1(6)	1.81	0.370	0.044	0.098	.2649	7.42	2.83	14,566
G-1(8)	1.81	0.366	0.051	0.102	.2787	6.74	2.83	9,936
G-2(1)	1.81	0.362	0.052	0.125	.3453	6.04	2.83	11,179
G-2(3)	1.81	0.356	0.046	0.103	.2893	5.76	2.83	10,266
G-2(4)	1.81	0.362	0.030	0.080	.2210	4.36	2.83	9,180
G-2(5)	1.81	0.382	0.035	0.080	.2094	6.64	2.83	12,427
G-2(6)	1.81	0.377	0.054	0.101	.2679	8.74	2.83	12,861
G-2(8)	1.81	0.379	0.053	0.096	.2533	8.65	2.83	11,025
G-3(1)	1.81	0.344	0.046	0.107	.3110	5.18	2.83	10,321
G-3(2)	1.81	0.348	0.042	0.100	.2874	5.04	2.83	10,017

MULLITE (cont.)

Sample Number	L	d	b	c	c/d	p	ρ	Fracture Surface Energy
G-3(3)	1.81"	0.349"	0.036"	0.091"	.2607	7.78#	2.83	28,073 ergs/cm^2
G-3(4)	1.81	0.334	0.046	0.092	.2754	5.98	2.83	12,564
G-3(5)	1.81	0.336	0.042	0.102	.3036	7.70	2.83	28,329
G-3(6)	1.81	0.332	0.048	0.089	.2681	5.90	2.83	11,017
G-3(7)	1.81	0.332	0.037	0.093	.2801	4.64	2.83	12,202
G-3(8)	1.81	0.332	0.048	0.096	.2892	6.90	2.83	16,793

(Crack width for all specimens = 0.010")

99.5% ALUMINA (ALSIMAG #753)

Sample Number	L	d	b	c	c/d	p	ρ	Fracture Surface Energy
1(I-1)	1.67"	0.381"	0.032"	0.140"	.3675	8.18#	3.87	17,193 ergs/cm^2
2(I-1)	1.90	0.382	0.017	0.056	.1466	7.45	3.87	19,687
3(I-1)	1.90	0.372	0.022	0.134	.3602	5.32	3.87	20,881
4(I-1)	1.90	0.388	0.020	0.125	.3222	5.54	3.87	19,750
6(I-5)	1.90	0.354	0.020	0.139	.3927	2.95	3.92	10,764
7(I-5)	1.90	0.351	0.021	0.046	.1311	7.45	3.92	15,027**
8(I-5)	1.90	0.350	0.023	0.130	.3714	5.18	3.92	23,208
9(I-5)	1.90	0.346	0.020	0.119	.3439	4.80	3.94	23,657
10(I-5)	1.90	0.351	0.021	0.126	.3590	3.84	3.92	14,203
12(I-4)	1.90	0.326	0.026	0.059	.1810	7.74	3.84	18,443
13(I-4)	1.90	0.329	0.018	0.112	.3404	3.70	3.84	19,930
14(I-4)	1.90	0.328	0.023	0.119	.3628	4.18	3.84	13,693

** Crack width 0.010" -- all others 0.028-0.030"

99.5% ALUMINA (cont.)

Sample Number	L	d	b	c	c/d	p	ρ	Fracture Surface Energy
15(I-4)	1.90"	0.333"	0.025"	0.030"	.0901	9.47#	3.84	14,234 ergs/cm^2**
16(I-2)	1.90	0.064	0.023	0.033	.0907	10.30	3.84	15,210
19(I-3)	1.90	0.352	0.018	0.063	.1790	6.28	3.90	19,725
21(I-3)	1.90	0.359	0.019	0.122	.3398	3.96	3.90	15,578
22(I-3)	1.90	0.348	0.025	0.119	.3420	4.68	3.90	13,994
23(I-3)	1.90	0.354	0.024	0.125	.3521	4.71	3.90	15,454
24(I-2)	1.67	0.362	0.016	0.028	.0773	8.15	3.84	13,280

** Crack width 0.010" -- all others 0.028-0.030"

99% ALUMINA (AD-99)

Sample Number	L	d	b	c	c/d	p	ρ	Fracture Surface Energy
F-1(2)	1.81"	0.314"	0.028"	0.090"	.2866	6.74#	3.86	22,210 ergs/cm^2
F-1(3)	1.81	0.312	0.039	0.078	.2500	11.36	3.86	27,451
F-1(4)	1.81	0.314	0.028	0.083	.2643	7.78	3.86	26,384
F-1(5)	1.81	0.305	0.034	0.081	.2656	9.54	3.86	29,651
F-1(6)	1.81	0.308	0.037	0.083	.2695	9.68	3.86	25,512
F-1(7)	1.81	0.309	0.028	0.065	.2104	8.12	3.86	22,655
F-1(8)	1.81	0.306	0.036	0.070	.2288	9.94	3.86	23,411
F-2(1)	1.81	0.329	0.038	0.075	.2280	13.14	3.86	29,171
F-2(2)	1.81	0.331	0.045	0.084	.2538	14.56	3.86	28,736
F-2(3)	1.81	0.329	0.034	0.056	.1702	9.38	3.86	13,351
F-2(4)	1.81	0.329	0.038	0.062	.1884	12.70	3.86	21,854
F-2(5)	1.81	0.341	0.026	0.081	.2375	6.68	3.86	15,153
F-2(6)	1.81	0.344	0.032	0.074	.2151	12.85	3.86	31,937
F-2(7)	1.81	0.341	0.020	0.075	.2199	6.30	3.86	20,734

99% ALUMINA (cont.)

Sample Number	L	d	b	c	c/d	p	ρ	Fracture Surface Energy
F-2(8)	1.81"	0.341"	0.027"	0.074"	.2170	11.18#	3.86	35,259 ergs/cm^2
F-3(1)	1.81	0.343	0.033	0.071	.2070	10.70	3.86	20,087
F-3(2)	1.81	0.340	0.042	0.072	.2118	11.22	3.86	14,389
F-3(4)	1.81	0.342	0.039	0.082	.2398	11.13	3.86	18,760
F-3(5)	1.81	0.350	0.034	0.070	.2000	9.08	3.86	12,305
F-3(6)	1.81	0.347	0.026	0.058	.1671	11.52	3.86	28,642
F-3(7)	1.81	0.348	0.038	0.090	.2586	13.86	3.86	32,049
F-3(8)	1.81	0.345	0.021	0.093	.2696	7.38	3.86	32,348

(Crack width for all specimens = 0.010")

96% ALUMINA (ALSIMAG #614)

Sample Number	L	d	b	c	c/d	p	ρ	Fracture Surface Energy
1(A-3)	1.67"	0.424"	0.064"	0.087"	.2052	35.62#	3.75	26,659 ergs/cm^2
2(A-3)	1.90	0.427	0.029	0.077	.1803	13.62	3.75	21,063
3(A-3)	1.90	0.426	0.040	0.079	.1854	17.05	3.75	18,010
4(A-3)	1.90	0.428	0.030	0.068	.1589	14.10	3.75	18,357
5(A-10)	1.90	0.392	0.043	0.145	.3699	9.64	3.74	17,059
7(A-10)	1.90	0.394	0.036	0.055	.1396	18.95	3.74	26,140
8(A-2)	1.90	0.302	0.072	0.061	.2020	36.60	3.78	81,864**
9(A-2)	1.67	0.398	0.058	0.093	.2337	19.00	3.78	13,105
10(A-2)	1.90	0.418	0.056	0.072	.1722	22.49	3.78	15,668
11(A-2)	1.90	0.416	0.040	0.036	.0865	27.25	3.78	23,786
12(A-2)	1.67	0.395	0.068	0.101	.2557	27.75	3.78	23,377
13(A-2)	1.90	0.370	0.062	0.095	.2568	20.60	3.78	24,986

** Very poor specimen (value discarded)

96% ALUMINA (cont.)

Sample Number	L	d	b	c	c/d	p	ρ	Fracture Surface Energy
14(A-2)	1.90"	0.418"	0.030"	0.049"	.1172	16.70#	3.78	20,641 ergs/cm^2
15(A-1)	1.90	0.344	0.028	0.066	.1919	8.51	3.75	18,417
16(A-1)	1.90	0.394	0.047	0.087	.2208	14.60	3.75	14,854
17(A-1)	1.90	0.383	0.064	0.076	.1984	24.30	3.75	21,395
19(A-1)	1.90	0.397	0.062	0.090	.2268	21.40	3.75	18,493

(Crack width for all specimens = 0.028-0.030")

94% ALUMINA (ALSIMAG #771)

Sample Number	L	d	b	c	c/d	p	ρ	Fracture Surface Energy
1(B-1)	1.90"	0.363"	0.030"	0.051"	.1405	12.90#	3.63	25,659 ergs/cm^2
2(B-1)	1.90	0.347	0.041	0.078	.2248	11.97	3.63	22,559
3(B-1)	1.67	0.365	0.030	0.056	.1534	13.10	3.63	21,682
4(B-1)	1.90	0.330	0.036	0.077	.2333	9.92	3.63	24,599
5(B-1)	1.67	0.364	0.052	0.098	.2692	19.14	3.63	29,802
6(B-2)	1.67	0.384	0.062	0.090	.2344	27.26	3.64	30,947
7(B-2)	1.67	0.384	0.080	0.087	.2266	33.30	3.64	25,818
8(B-2)	1.67	0.403	0.046	0.125	.3102	12.11	3.64	13,739
9(B-3)	1.90	0.407	0.069	0.083	.2039	30.00	3.66	27,217
10(B-5)	1.90	0.364	0.038	0.088	.2418	13.60	3.66	27,321
11(B-5)	1.90	0.365	0.037	0.026	.0712	25.87	3.66	30,456
13(B-5)	1.90	0.374	0.034	0.027	.0722	22.28	3.66	25,124
14(B-5)	1.90	0.372	0.039	0.027	.0726	24.25	3.66	23,108
15(B-5)	1.90	0.372	0.029	0.059	.1586	12.34	3.66	22,440

94% ALUMINA (cont.)

Sample Number	L	d	b	c	c/d	p	ρ	Fracture Surface Energy
17(B-5)	1.90"	0.369"	0.029"	0.027"	.0732	14.87#	3.66	16,227 ergs/cm^2
18(B-13)	1.90	0.352	0.033	0.026	.0739	17.70	3.63	24,243
19(B-13)	1.90	0.342	0.046	0.164	.4795	7.21	3.63	26,858
20(B-13)	1.90	0.343	0.038	0.026	.0758	18.63	3.63	22,439
21(B-13)	1.90	0.344	0.034	0.050	.1453	11.32	3.63	18,783
22(B-13)	1.90	0.350	0.030	0.035	.1000	14.50	3.63	26,353

(Crack width for all specimens = 0.028-0.030")

APPENDIX D

MATERIALS AND THEIR SUPPLIERS

D-1. Donated Materials:

The 99.5, 96 and 94% aluminas, the steatite and zircon were donated by: THE AMERICAN LAVA CORPORATION
Chattanooga, Tennessee 37045
through the efforts of Dr. Joe Bailey.

The mullite rods were donated by:

MC DANEL REFRACTORY PORCELAIN CO.
510 Nineth Avenue
Beaver Falls, Pennsylvania 15010

The "HITEC" high temperature heat transfer salt was donated by:

I. E. duPONT deNEMOURS & CO., INC.
Explosives Department
Wilmington, Delaware

D-2. Other Materials Used in Work:

Diamond Saw Blades (as thin as 0.012"):

CHAPMAN KNIVES & SAWS
3366 Tree Court Industrial
St. Louis, Missouri

Wire Saw Blades and Abrasive:

SOUTH BAY TECHNOLOGY
4900 Double Drive
El Monte, California 91731

Load Cell and Charge Amplifier:

KISTLER INSTRUMENT CORPORATION
Clarence, New York

VIII. BIBLIOGRAPHY

1. AINSWORTH, John, "The Damage Assessment to Thermal Shocked High Density, High Purity Alumina," Ph.D. Dissertation, University of Missouri-Rolla Library, Rolla, Missouri, 1968.

2. DAVIDGE, R. W. and TAPPIN, G., "The Effective Surface Energy of Brittle Materials," J. Mat'ls. Science, 3, 165-73 (1968).

3. SUMMERS, David A., et al., "A Comparison of Methods for the Determination of Surface Energy," Proc. - 12th Symposium on Rock Mechanics, November 1970.

4. SRAWLEY, John E., "Plane Strain Fracture Toughness," Fracture, Leibowitz, Ed. (New York: Academic Press, 1969) 4, 45-68.

5. CHEN, Li-King, "Surface Energy Determinations in Plexiglas," M.S. Thesis, University of Missouri-Rolla Library, Rolla, Missouri, 1970.

6. WULFF, J., ROSE, M., et al., "Thermodynamics of Structure," The Structure and Properties of Materials (New York: John Wiley & Sons, Inc., 1966) 2, Chap. 3, 46-59.

7. STEWART, G. H., "Science of Ceramics," pub. by The British Ceramic Society (London and New York: Academic Press, 1965) 2.

8. WEIDERHORN, S. M., "Fracture in Ceramics," Mech. and Therm. Prop. of Ceramics, J. B. Wachman, Jr., Ed. (NBS Special Pub. 303, May 1969).

9. TATTERSALL, H. G. and TAPPIN, G., "The Work of Fracture and Its Measurement in Metals , Cer. and Other Mat'ls.," J. Mat'ls. Sci., 1, 296-301 (1966).

10. ALLEN, B. C., "The Surface Tension of Liquid Transition Metals at Their Melting Points," Trans. Met. Soc. AIME, 227, 1175-83 (Oct. 1963).

11. KENNY, William J., "Energy-New Surface Relationship in the Crushing of Solids-Slow Compression Crushing of Single Particles of Glass," Ph.D. Dissertation, University of Minnesota, 1957.

12. PICKETT, Gerald, "Equations for Computation of Elastic Constants from Flexural and Tortional Resonant Frequencies of Vibration of Prisms and Cylinders," ASTM Proceedings, 45, 846-59 (1945).

13. WEIDERHORN, S. M., "Crack Propogation in Polycrystalline Ceramics," Ultra-fine-grained Ceramics (New York: Syracuse University Press, 1970).

IX. VITA

Gene Arthur Pahlmann was born on July 27, 1946, in Alton, Illinois. He was the first of three sons born to Mr. and Mrs. Herman W. Pahlmann. His grade-school education took place in Roxana and Alton, Illinois, Fort Wayne, Indiana and finally Wood River, Illinois, where he entered Junior High School and graduated from High School on June 6, 1964. In September of 1964 he entered the University of Missouri-Rolla as a freshman in Ceramic Engineering. On January 19, 1969, he received his Bachelor of Science in Ceramic Engineering and also a commission as Second Lieutenant in the United State Army Reserve.

His college education was financed through the generous help of his father and by working during the summers on cross-country natural gas pipeline construction.

In January of 1969 he enrolled as a special student in the graduate school at the University of Missouri-Rolla. In February of 1970 he received a fellowship from the Refractories Institute, which lasted through the following September, while he worked on his Master of Science in Ceramic Engineering.

His academic interests lie not only in the field of ceramics, where colored glasses are his greatest interest, but also in the fields of explosive research and polymers.